

See discussions, stats, and author profiles for this publication at:  
<https://www.researchgate.net/publication/259095786>

# Design and development of fluorescent nanostructures for bioimaging

ARTICLE *in* PROGRESS IN POLYMER SCIENCE · JANUARY 2013

Impact Factor: 26.93 · DOI: 10.1016/j.progpolymsci.2013.11.001

---

CITATIONS

50

---

READS

346

## 2 AUTHORS, INCLUDING:



Meizhen Yin

Beijing University of Chemical Technol...

112 PUBLICATIONS 598 CITATIONS

SEE PROFILE



# Design and development of fluorescent nanostructures for bioimaging

Mengjun Chen, Meizhen Yin\*

*State Key Laboratory of Chemical Resource Engineering, Key Laboratory of Carbon Fiber and Functional Polymers, Beijing University of Chemical Technology, Beijing 100029, China*

## ARTICLE INFO

### Article history:

Received 28 June 2013

Received in revised form 1 November 2013

Accepted 5 November 2013

Available online 9 November 2013

### Keywords:

Bioimaging

Fluorescence

Nanostructures

Structural design

Sensitivity

Selectivity

## ABSTRACT

Because fluorescence-based techniques are inherently sensitive, selective, convenient, diverse, non-destructive, potentially real time and *in situ*, they have been widely used in biological imaging. Especially those, with specific fluorescent nanostructures (FNSs) as detecting media in bioimaging, have already been intensively studied for more than a decade because of the convenient transduction of optical signal, high sensitivity and rapid response of FNSs. In this review, we summarize the major strategies to design FNSs with specific structures for biological imaging. First, recent advances are briefly introduced. Then, the specific design of FNSs and their applications are reviewed, in which their fluorescence mechanism, strategies in designing and development, preparation methods, and some representative applications in bioimaging are described. Finally, future perspectives and ongoing issues of FNSs and their applications in bioimaging are discussed. Although many FNSs have been synthesized and applied biologically, many studies still should be done before they can be widely employed as fluorescent probes in clinical tests. With further advances in design and synthesis of high quality multifunctional FNSs, the widespread application of FNSs may be expected not only in advanced bioimaging, but also in ultra-sensitive molecular diagnosis, novel light-emitting nanodevices and intracellular drug delivery.

© 2013 Elsevier Ltd. All rights reserved.

## Contents

1. Introduction .....	366
2. Organic fluorescent nanostructures .....	367
2.1. Carbon-based fluorescent nanostructures .....	367
2.2. Fluorescent macromolecules .....	369
2.2.1. Fluorophore doped macromolecules .....	369
2.2.2. Intrinsic-fluorescent macromolecules .....	370
2.3. Fluorescent polymeric nanoparticles .....	371
2.4. Fluorescent supermacromolecular nanoassemblies .....	373
2.5. Aggregation-induced emission fluorophores .....	375
3. Inorganic fluorescent nanostructures .....	376
3.1. Quantum dots .....	376
3.2. Silicon nanoparticles .....	379
3.3. Fluorescent metallic nanoclusters .....	379

\* Corresponding author.

E-mail address: [yinmz@mail.buct.edu.cn](mailto:yinmz@mail.buct.edu.cn) (M. Yin).



3.4.	Complexed inorganic fluorescent nanostructures.....	380
3.4.1.	Upconversion nanoparticles .....	380
3.4.2.	Inorganic core/shell fluorescent nanoparticles .....	382
4.	Organic/inorganic hybrid fluorescent nanostructures .....	383
4.1.	Inorganic@organic hybrid fluorescent nanostructures .....	383
4.2.	Organic@inorganic hybrid fluorescent nanostructures .....	384
4.3.	Heavy-metal complex.....	385
5.	Perspective.....	386
6.	Summary.....	387
	Acknowledgements .....	387
	References .....	387

## Nomenclature

AAc	acrylic acid
ACQ	aggregation-caused quenching
AS-ODN	antisense oligonucleotide
ATRP	atom transfer radical polymerization
BODIPY	boron-dipyrromethene
BRET	bioluminescent resonance energy transfer
COPV	1,4-dimethoxy-2,5-di [4'- (cyano)styryl]benzene
CQD	carbon quantum dot
DMAEMA	2-dimethylamino ethyl methacrylate
DSA	9,10-distyrylanthracene
DSB	1,4-distyrylbenzene
ECM	extracellular matrix
FA	folic acid
FCNP	fluorescent capsid nanoparticle
FNS	fluorescent nanostructure
FRET	fluorescence resonance energy transfer
FQY	fluorescence quantum yield
GMA	glycidyl methacrylate
GQD	graphene quantum dot
HBC	hexa-peri-hexabenzocoronene
HCP	hyperbranched conjugated polymer
HEMA	2-hydroxyethyl methacrylate
LBL	layer-by-layer
LRP	living radical polymerization
MEF	mouse embryonic fibroblast
MMA	methyl methacrylate
MNP	magnetic nanoparticle
NC	nanocluster
NIPAM	<i>N</i> -isopropylacrylamide
NIR	near-infrared
NMRP	nitroxide mediated radical polymerization
NP	nanoparticle
NVK	<i>N</i> -vinylcarbazole
PAMAM	poly(amidoamine)
PBS	phosphate buffered solution
PCPE	phosphorescent conjugated polyelectrolyte
PDI	perylene diimide
PEBBLE	probe encapsulated by biologically localized embedding
PEGMA	poly(ethylene glycol)methacrylate
PGD	polyglycerol dendrimer

PS	polystyrene
QD	quantum dot
RAFT	reversible addition-fragmentation chain transfer
RE	rare earth
RhB	rhodamine-B
SiNP	silicon nanoparticle
SWNT	single walled carbon nanotube
TPA	triphenylamine
TPE	tetraphenylethene
TPF	two-photon fluorescence
TTA	triplet-triplet annihilation
UCNP	upconversion nanoparticle
UV	ultraviolet
VBC	4-vinylbenzyl chloride

## 1. Introduction

Biological imaging (bioimaging) has become a powerful tool in biological research today because it offers an unique approach to visualize the morphological details of cells [1]. To date, fluorescence-based techniques have been greatly encouraged in bioimaging due to their inherent superiorities, such as high sensitivity, high selectivity, convenience, diversity and non-destructive character [2]. Typically, fluorescent probes are exploited to label the target with specific chemical structures and thus to generate fluorescent signals during the fluorescence-based bioimaging. Since nanostructure-based detection platforms can provide many advantages over traditional approaches in terms of sensitivity, signal stability and multiplexing capability, a growing interest has been shown recently in the design of different fluorescent nanostructures (FNSs) as fluorescent probes in bioimaging [3–6]. Currently, the most studied FNSs in bioimaging include fluorescent proteins, organic dyes, metal complexes, semiconductor nanocrystals, and upconversion nanophosphors [7–10]. In order to obtain a better fluorescent probe, further works on FNSs with recommended chemical and optical properties have also been reported. For example, surface modification of FNSs has been done with bright fluorescence, high photostability, large Stokes shift and flexible processability in order to be further conjugated with biomolecules and/or fluorophores [6].

In this review, classification of FNSs, their fluorescence mechanisms and applications in bioimaging are summarized. According to the compositions and structures of FNSs, they are divided into three classifications, i.e., organic FNSs, inorganic FNSs and organic/inorganic hybrid FNSs (Fig. 1). Based on the classification of FNSs, their design strategies, fluorescing mechanisms, size-dependent optical properties and preparing methods are introduced and discussed. Especially, their representative applications in bioimaging at the cell- and tissue-levels are reviewed. Furthermore, potentials of FNSs and their perspectives in the field of bioimaging, based on their advantages and security, are discussed.

## 2. Organic fluorescent nanostructures

Among all of the FNSs used in bioimaging, organic FNSs are the most widely studied due to their rich chemical structures, easy chemical modification and high fluorescence quantum yield (FQY) [11,12]. Generally, these organic FNSs include carbon-based fluorescent nanostructures, fluorescent macromolecules, fluorescent polymeric nanoparticles, fluorescent supermacromolecular nanoassemblies and aggregation-induced emission fluorophores.

### 2.1. Carbon-based fluorescent nanostructures

Carbon-based FNSs are the basic organic fluorescent materials with only carbon elements and are currently one of the most attractive nanomaterials with different forms, such as fullerenes, single- and multiple-walled carbon nanotubes, carbon nanoparticles, nanofibers, and so forth. Such carbon-based FNSs have become important

due to their unique chemical and physical properties (*i.e.*, good thermal and electrical conductivity, high mechanical strength and optical properties), which are essential in many biomedical areas, such as bioimaging, drug delivery, tissue scaffold reinforcements, and cellular sensors [13]. However, these carbon-based nanomaterials show size-dependent toxicity. Moreover, cytotoxicity is enhanced when their surface is functionalized after an acid treatment. Therefore, further effort should be made on carbon-based FNSs [14].

Recently, zero-dimensional carbon-based FNSs, such as carbon quantum dots (CQDs) [15–18] and graphene quantum dots (GQDs) [19,20], have aroused great interest in bioimaging due to their strongly multiphoton-fluorescence and extremely large two-photon crosssections on pulsed laser excitation (800–900 nm) [21,22]. For example, Yang et al. [22] prepared nontoxic fluorescent CQDs with surface-passivation by oligomeric PEG<sub>1500N</sub>. In addition to the apparent biocompatibility, CQDs exhibited competitive (on the order of magnitude, at least) fluorescence imaging performance to that of the commercial CdSe/ZnS QDs (introduced in the following), demonstrating their potentials for both *in vitro* and *in vivo* applications. Similarly, Qian et al. [23] synthesized a series of functionalized GQDs with different small organic molecules (dialcohols, diamines and dithiols). By altering size and surface functionalization of GQDs, effective modulation of their photoluminescence could be achieved, which could render great performance of GQDs in HeLa cell bioimaging. Since many reviews have been published on the advantages of such zero-dimensional carbon-based FNSs in bioimaging [24–26], they will not be discussed extensively in this review.

Compared with the materials mentioned above, carbon nanotubes have shown unique optical properties

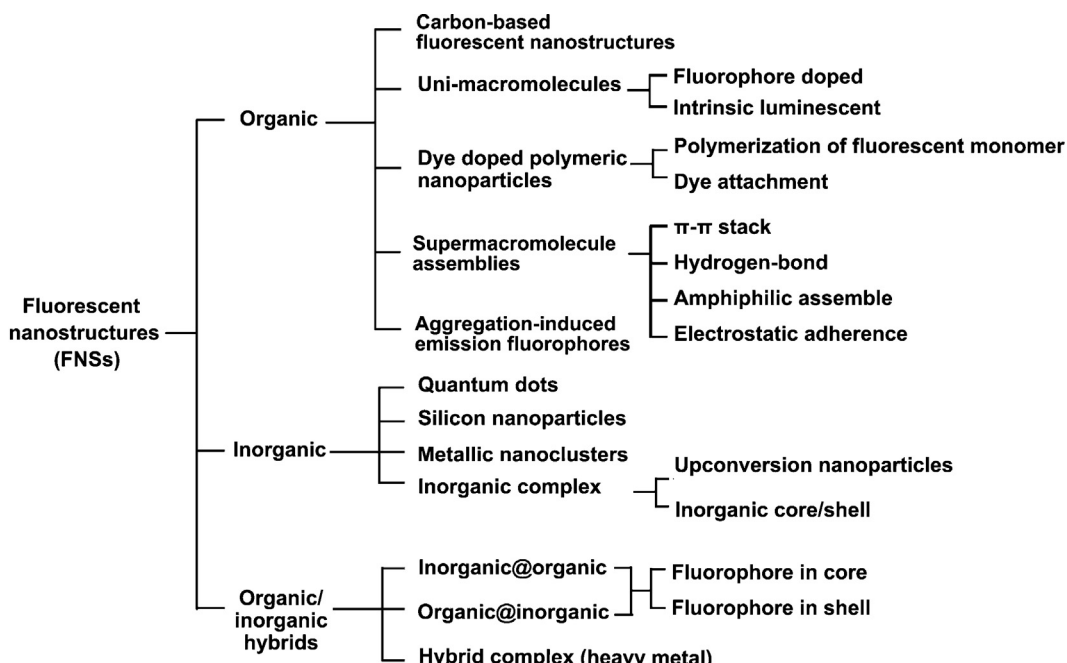


**Fig. 1.** Classification of fluorescent nanostrucutures (FNSs) based on their different chemical structural compositions.

in biological application [27–29]. Single walled carbon nanotubes (SWNT) are upcoming potential candidates for the fluorescence imaging agents because they generate fluorescence brightly in the 800–1600 nm wavelength range of the near-infrared (NIR) region that has greater penetration depth and lower excitation scattering [30,31] ( $FQY = 1.7 \times 10^{-4}$ – $10^{-3}$ ), which has been shown very useful in biological tissue imaging. One key advantage of SWNTs is their ability to translocate through plasma membranes, allowing their use for the delivery of therapeutically active molecules in a manner that resembles cell-penetrating peptides [28]. As labeling or imaging agents, SWNTs are bright enough to allow image deep inside living body at high frame rate without excessive excitation power [32]. For example, Robinson et al. [33] demonstrated

the application of intravenously injected SWNTs as photoluminescent agents for *in vivo* tumor imaging in the 1.0–1.4  $\mu\text{m}$  emission region with a high tumor uptake of SWNTs, which is the first time to use the intrinsic NIR photoluminescence of SWNTs for tumor imaging.

Generally, fluorescence imaging of SWNTs provide powerful tools to trace the interactions of nanotubes with cells, tissues, and organisms. And the auto-fluorescence in the NIR region is much lower than that in the ultraviolet or visible ranges. These properties make SWNTs potential imaging agents with higher resolution and greater tissue depth for NIR fluorescence microscopy and optical coherence tomography. However, aggregation of nanotubes into bundles that quenches the fluorescence through interactions with metallic tubes and substantially broadens the

**Table 1**

The most reported organic dyes conjugated to fluorescent uni-macromolecules.

Small organic fluorophores	General structural formula	Refs.
Anthracene		[44]
Coumarin		[45–48]
BODIPY		[49–51]
Fluorescein		[52–56]
Rhodamine		[57–59]
Perylene bisimides		[60–65]
Cyanine		[66–71]
Donor- $\pi$ -acceptor or acceptor- $\pi$ -acceptor fluorenyl derivatives	 $R_1 = \text{C}_6\text{H}_4\text{CO}^- \text{O}^-, \text{C}_6\text{H}_4\text{CH}_2\text{Cl}, (\text{CH}_2=\text{CH})_n \text{H}, \text{C}_6\text{H}_4\text{C}_6\text{H}_{11}, \text{C}_6\text{H}_4\text{C}_6\text{H}_{12}\text{Cl}, \text{C}_6\text{H}_4\text{C}_6\text{H}_{12}\text{Br}, \text{C}_6\text{H}_4\text{C}_6\text{H}_{12}\text{I}, \text{C}_6\text{H}_4\text{C}_6\text{H}_{12}\text{NO}_2, \text{C}_6\text{H}_4\text{C}_6\text{H}_{12}\text{SO}_3^- \text{Na}^+$ 	[72–75]

$R_1$  = Donor or Acceptor,  $R_2$  = Acceptor

absorption spectra [34]. Therefore great effort should be needed to improve the dispersion of individual SWNT for better performance of SWNT in bioimaging.

## 2.2. Fluorescent macromolecules

A fluorescent macromolecule is an individual organic macromolecule that generates fluorescence after the absorption of excitation light. Depending on the fluorescent mechanism, fluorescent macromolecules can be usually divided into two classes: (1) fluorophore-doped macromolecules and (2) intrinsic-fluorescent macromolecules.

### 2.2.1. Fluorophore doped macromolecules

A fluorophore-doped macromolecule is a unimolecular nanostructure with organic fluorophores. And the fluorophores have been identified as small organic dye molecules or their derivatives with resonant emission [35–43], such as fluorescein, rhodamine, perylene, cyanines, boron-dipyrrromethene (BODIPY), and two-photon absorbing materials. The most often reported fluorophores are summarized in Table 1. And these macromolecules exhibited asymmetric emission spectra (400–700 nm, only a few NIR dyes could reach above 700 nm; FQY=0.5–1.0 (visible), 0.05–0.25 (NIR)) as the original fluorophores did.

The fluorophore-doped macromolecules, such as dendrimers and hyperbranched macromolecules (Fig. 2), were developed into core–shell structures *via* the following strategies [76,77]. The macromolecules could display the original fluorescence with the chromophores located in the core or the branch sites or the periphery. Meanwhile, the desired properties of probes, such as stability, biocompatibility, and specificity of labeling, would be obtained by grafting or growing the shell.

A dendrimer is a nanoscaled macromolecule with well-defined branching structure. Fluorescent dendrimer can be prepared with high regularity and controllable molecular weights, and it has a fluorophore-doped central core linked covalently to uniform repeating units (generations) and many terminal groups. Those well-defined dendrimers were reported as imaging agents in gene delivery system

[78–84], in which higher generation materials (G6 or G7) were required because low generation dendrimers could not condense siRNA into uniformly small complexes [85]. However, due to the increased toxicity of their growing generations [86], it is very important to improve the biocompatibility of dendrimers. Recently, Yin and co-workers [60] reported the preparation of G1, G2 and G3 of perylenedimide (PDI)-cored cationic dendrimer with peripheral amine groups, which could rapidly enter live cells with high gene transfection efficiency and low cytotoxicity (Fig. 3). Yang et al. [87] also synthesized monovalent probe on a ring-fused BODIPY core that is conjugated to a polyglycerol dendrimer (PGD), which has exhibited excellent brightness with an emission maximum at 705 nm.

Unlike dendrimers, fluorescent hyperbranched macromolecules suffer from difficulty in structural control, because its functional groups are located randomly, and not all the reactive sites in the repeat units have reacted. Compared with highly regular dendrimers, structural defects of fluorescent hyperbranched macromolecule offer better flexibility for its bioimaging applications, because both the branching arms and branching points could provide the reactive sites for the incorporation of functional groups. Among these fluorescent hyperbranched macromolecules, star polymers are the simplest branched material, with several linear polymer chains attached to a single branching point (core) [88–90]. The “core-first” method mostly starts from a fluorescent macro-initiator (core) and the well-defined architecture can be realized *via* living radical polymerization (LRP). Radical polymerization approach offers several advantages, especially in terms of compatibility with both aqueous and organic media as well as an excellent tolerance to many functional groups. LRP includes nitroxide mediated radical polymerization (NMRP) [91,92], reversible addition-fragmentation chain transfer (RAFT) polymerization [93–96], and atom transfer radical polymerization (ATRP) [97–99]. Among the reported LRP techniques, ATRP is most frequently used in the preparation of well-defined fluorescent star polymers. Yin and Müllen [100–105] reported several examples using this method. For example, they successfully synthesized a positively charged fluorescent core–shell dendritic star polymer [102]. They started with a macro-initiator with a central PDI chromophore and a first-generation polyphenylene dendrimer scaffold, then initiated the outer shell, which was consisted of eight-armed linear polymers with multiple amine groups (Fig. 4(a)R1). Such designed structure exhibited great water solubility and fluorescent property with positive charges, which could bind to the highly negatively charged extracellular matrix (ECM, Fig. 4(b)). Similarly, they synthesized a series of negatively charged dendritic star polymers with eight-armed linear polymers bearing multiple carboxyl groups (Fig. 4(a)R2), aiming at specifically staining the cell nucleus by binding to positively charged nuclear proteins (Fig. 4(c)) [105]. Additionally, some complicated fluorescent hyperbranched macromolecules have also been reported, in which the fluorophores could be conjugated in the branched arms [106] or cores [65] to achieve desired optical properties. Such structures offered more available strategies for site-specific covalent labeling of cells or tissues.

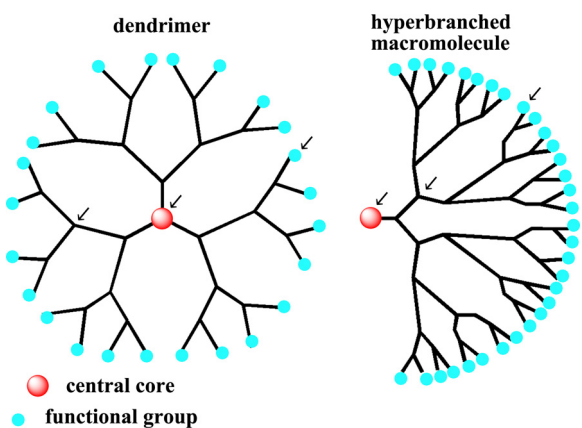


**Fig. 2.** Structures of fluorescent dendrimer and hyperbranched macromolecules. The chromophores could be in the central core or the branch sites or the periphery (indicated by arrows).

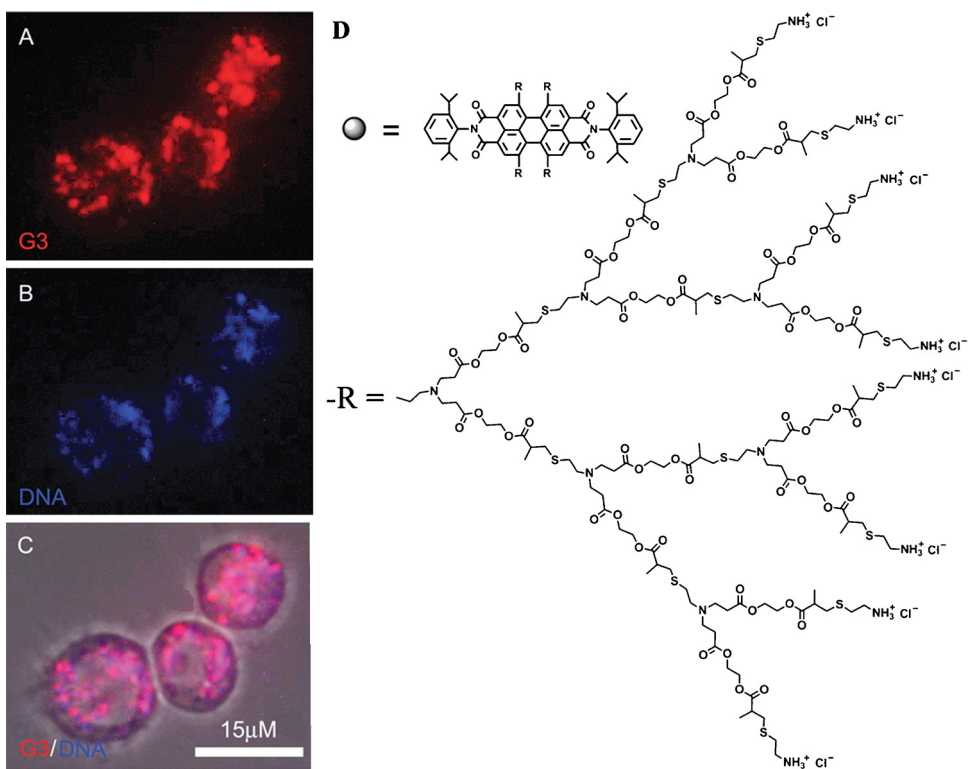


**Fig. 3.** Fluorescence images (a–c) of the G3-DNA complex inside of cells after 48 h of incubation. (a) G3 fluorescence image (red); (b) CXR reference dye labeled DNA (blue); (c) merged channels of (a) and (b); (d) structure of perylenediimide (PDI)-cored dendrimers [60]. Copyright 2013. (For interpretation of the references to color in this figure legend, the reader is referred to the web version of the article.) Adapted with permission from the Royal Society of Chemistry.

Generally, the optical property of fluorophore-doped macromolecule is attributed to the conjugated fluorophores, while its specific labeling capability is owing to the superficial functional groups. Moreover, the sizes of these macromolecules could be in the range of 1–20 nm [101], which are dependent on the designed structure and the chemical environment (pH, solvent, temperature, etc.). By tuning the polymer arms or the generation of macroinitiator, the size of the nanostructure could be controlled, which would further affect its performance in specific fluorescent

labeling in the following two ways [107,108]: (1) the fluorescence intensity of dendritic structure is determined by its generation; (2) higher dendron leads to larger size and offers more superficial functional groups to combine biological targets.

#### 2.2.2. Intrinsic-fluorescent macromolecules

An intrinsic-fluorescent macromolecule is a type of nanostructure that exhibits fluorescence (400–500 nm) without fluorophore conjugation ( $FQY = 0.025\text{--}0.98$ ).

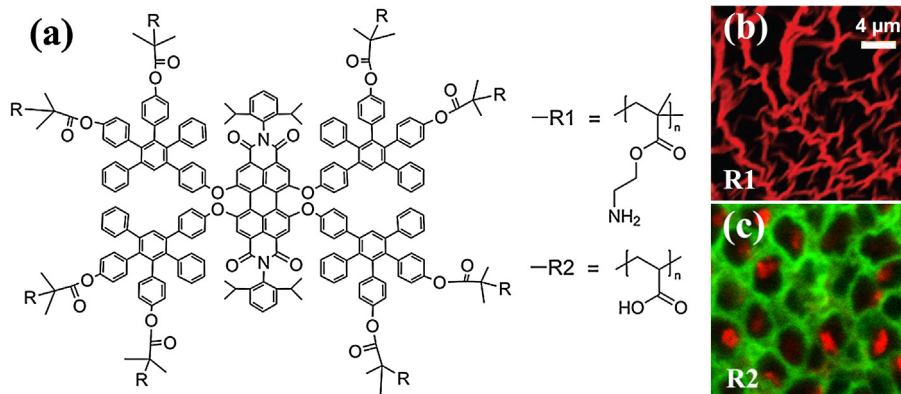


**Fig. 4.** (a) Structure of fluorescent core–shell dendritic star polymer (R1: positively charged, R2: negatively charged); (b) fluorescent image of R1 labeled extracellular matrix; (c) fluorescent image of R2 labeled nuclear proteins [102,105]. Copyright 2008. Reproduced, respectively, with permission from the American Chemical Society and Wiley-VCH Verlag GmbH & Co. KGaA, Weinheim.

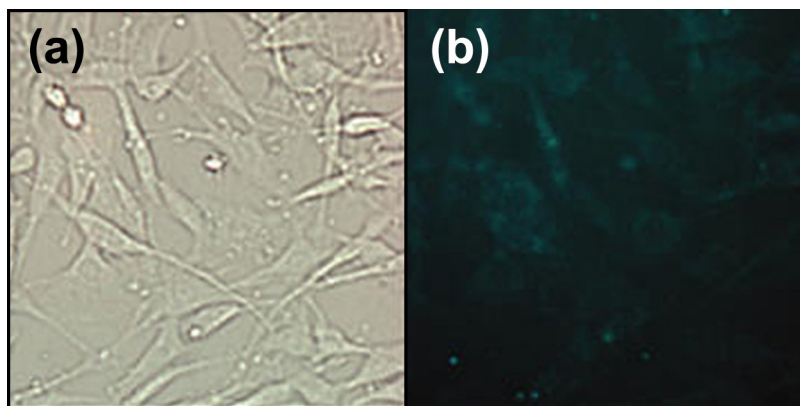


**Fig. 5.** (a) Optical and (b) fluorescence microscopic images of C6 cells transfected with the complex of fluorescent G4 PAMAM dendrimer and AS-ODN for 12 h [114]. Copyright 2011. Adapted with permission from the American Chemical Society.

Representative examples are dendrimers or hyperbranched macromolecules with aliphatic tertiary amine, such as the hyperbranched poly(amine-ester), poly(amidoamine) (PAMAM), poly(propyletherimine) dendrimers and so on [109–113]. Since these FNSs are considered as biocompatible, nonimmunogenic and water-soluble gene vehicles, they exhibit many potential advantages in bio-applications. For example, Tsai et al. [114] successfully synthesized PAMAM dendrimers with numerous primary amines on the surface. The dendrimers with intrinsic blue fluorescence obtained were used to monitor the gene delivery and transfection toward rat C6 glioma cells directly. They also combine antisense oligonucleotides (AS-ODN) with PAMAM dendrimers electrostatically to knock down specific protein expressions. Based on fluorescence of the resulted PAMAM–(AS-ODN) complexes, the uptake process could be evaluated directly via fluorescence techniques (Fig. 5). As new fluorescent probe materials in bioimaging, intrinsic-fluorescent macromolecules attracted substantial interest to understand their luminous mechanism. However, fluorescence of these FNSs can be quenched easily and strong fluorescence has been observed only in vapor phase. Therefore, Pan and his co-workers [115–117] made great effort to retain the strong fluorescence of these FNSs. Although intrinsic-fluorescent macromolecules have been extensively studied [118,119], so far the intrinsic-fluorescent mechanism has not been studied systematically.

### 2.3. Fluorescent polymeric nanoparticles

Dye-doped polymer nanoparticles (NPs) are cross-linked polymeric spheres in which fluorescent dyes were covalently attached or physically entrapped. Typically, these FNSs were synthesized through the copolymerization of fluorescent monomers with other functional monomers [120–126] or the encapsulation of fluorescent organic dye molecules inside or on the matrix (Fig. 6) [127–130]. Because of polymeric NPs supports (with sizes of ~100 nm), the composite FNSs exhibit good biocompatibility, controllable morphology and original optical property of the doped dye.

By using fluorescent monomer, the required optical properties could be introduced into the product after the polymerization. Because the chromophore was incorporated in the particle *via* chemical bond, the resulted FNPs had good stability and desired fluorescence. For instance, Marco et al. [131] synthesized a fluorescent monomer *via* binding the fluorescent dye Rhodamine-B (RhB) and 2-hydroxyethyl methacrylate (HEMA) covalently, then produced fluorescent NPs *via* the free radical emulsion copolymerization of the fluorescent monomer with methyl methacrylate (MMA) for bioimaging. Similarly, Sauer et al. [132] synthesized a fluorescent surfmer (surfactant monomer) by combining surface activity, polymerizability and fluorescent property within one molecule. By using the fluorescent surfmer, fluorescent surface-labeled polystyrene (PS) NPs were synthesized *via* miniemulsion polymerization. This approach could offer the potential to size-controlled fluorescent NPs by using specific polymerization. In addition, the steric hindrance of polymeric nanoparticle should be considered during the material design and the analysis of properties.

Due to the limited number of fluorescent monomers for polymerization, other better ways are still being explored

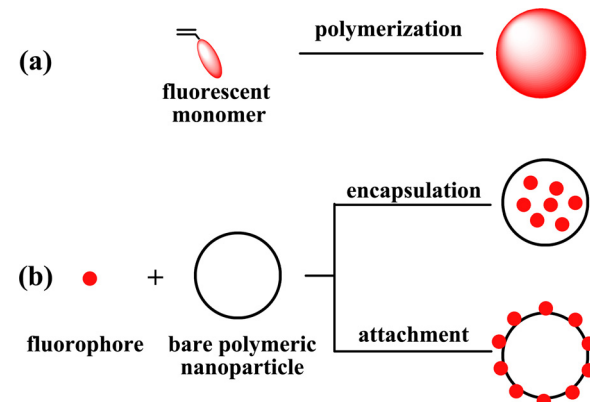


**Fig. 6.** Two strategies toward fluorescent polymeric nanoparticles: (a) polymerization of fluorescent monomers; (b) encapsulating fluorophores inside or attaching fluorophores onto the bare polymeric nanoparticles.

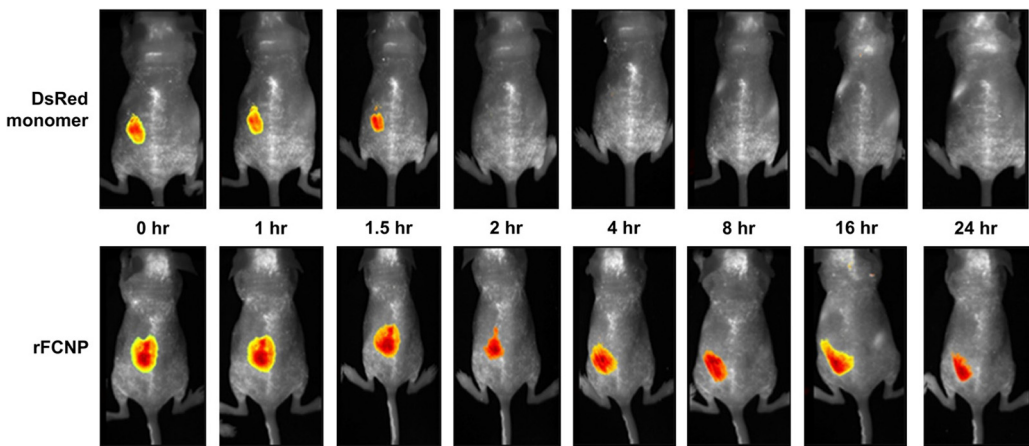


**Fig. 7.** Estimation of *in vivo* stabilities of rFCNP and DsRed that are subcutaneously injected into BALB/cSlc-*nu* mice (female 4 weeks old, JAPAN SLC, Inc.) [133]. Copyright 2012.  
Reproduced with permission from Elsevier Ltd.

to synthesize NPs with good fluorescent properties. Wherein, the bare polymeric NPs with desired sizes were prepared first and then the combination of dyes was realized to achieve their fluorescence *via* chemical cross-links. Due to the chemical cross-links, the composite FNSs were very stable, but special functional groups were required for the integration between NPs and fluorophores. Varied sized fluorescent polymeric NPs could have different kinetic profiles, uptake and distribution rates, *etc*. Therefore, multifunctional FNSs were developed on the basis of various support polymeric materials. Yoo et al. [133] synthesized hepatitis B virus capsid particles and genetically grafted fluorescent protein (DsRed or eGFP) onto their surface, which resulted in the construction of red or green

fluorescent capsid nanoparticles (FCNPs). Because of the *in vivo* high stability inside of mice, such FCNPs seemed to have a great potential as an effective and non-cytotoxic tool for *in vivo* optical imaging, compared with the single fluorescent protein monomer (Fig. 7). Certainly, these FNSs might expose the fluorophores in external environment, causing fluorophore oxidation or photobleaching, thus their photostability could not be improved.

In the physical interaction, fluorescent molecules were usually directly involved inside the matrix NPs without any chemical interaction. The polymeric NPs acted as a protecting agent to improve the stability and compatibility of the FNSs in the physiological environment. In this way, hydrophobic fluorophores could also be considered

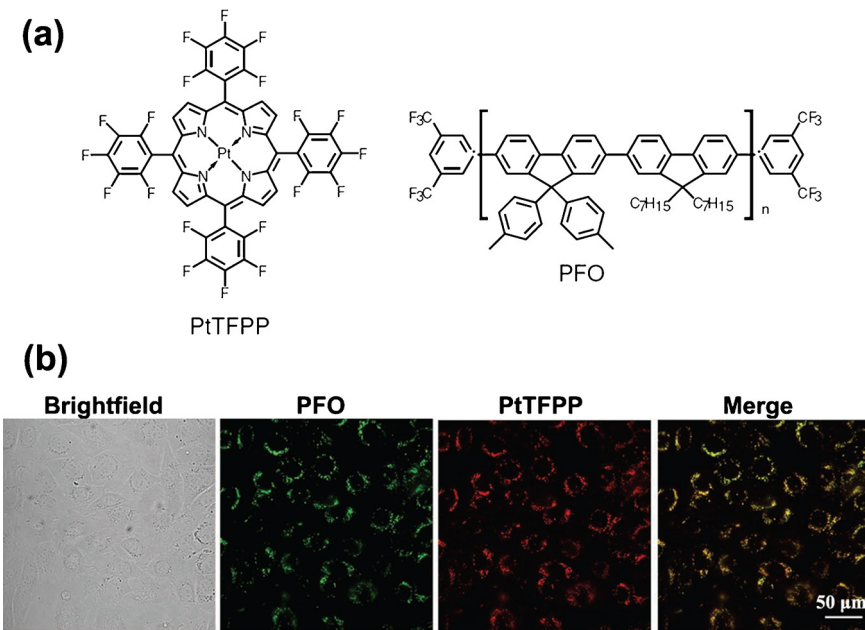


**Fig. 8.** (a) Chemical structures of phosphorescent PtTFPP reporter and PFO; (b) fluorescent images of MEF cells stained with MM2 (10 g/mL, 16 h) [136]. Copyright 2012.  
Reproduced with permission from WILEY-VCH Verlag GmbH & Co. KGaA, Weinheim.

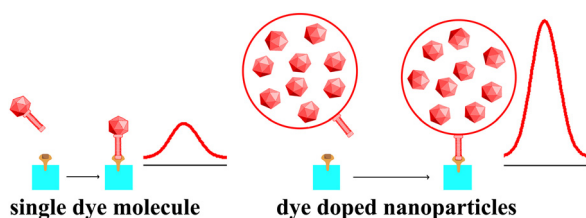


**Fig. 9.** The process of specific labeling and the comparison of fluorescence intensity between single dye molecule and dye-doped nanoparticles.

in bioimaging through encapsulation within hydrophilic polymeric NPs. Dye-doped NPs *via* physical method were probes encapsulated by biologically localized embedding (PEBBLE) and widely used as probes for bio-sensing and imaging in live cells [134,135]. For example, Kondrashina et al. [136] reported a new cell-penetrating phosphorescent nanosensor material, MM2 probe, by embedding the following two novel dyes into cationic hydrogel NPs: (1) phosphorescent reporter dye, PtTFPP (Fig. 8(e)); (2) O<sub>2</sub>-insensitive reference fluorophore (PFO, Fig. 8(e)) as one- and two-photon light harvesting antennae and fluorescence resonance energy transfer (FRET) donor for PtTFPP. The formed PEBBLEs (MM2) were applied in sensing and imaging of (intra)cellular oxygen of mouse embryonic fibroblast (MEF) (Fig. 8(a)–(d)). The procedure did not require any special functionality of doped dyes as long as they had enough affinity to the involved polymeric NPs. However, without covalent binding between the fluorophore and the matrix, dye molecules can be disassociated from the particles over time, which decreases per-particle brightness and increases the background signal. Therefore it is a challenge to improve the photostability of the fluorescent NPs by physical methods.

Generally, during inserting the fluorescent dye into matrix NPs by covalent attachment or physical entrapment to produce designed fluorescent polymeric NPs, the size of every individual FNS was determined by the size of the supporting polymeric NP, and the size-independent optical property was related to the type and the amount of incorporated fluorophores. The polymer section of the composites, either as matrix or protecting agent, contributes to the uniform distribution of the involved fluorophores, which could efficiently avoid quenching or photobleaching. Compared with fluorescent macromolecules, fluorescent polymeric NPs obtained from these procedures could produce a highly amplified optical signal (Fig. 9) due to the incorporation of several dye molecules. Although quantification of the doped fluorophores couldn't be accurately controlled in each NP, it did not exhibit any obvious negative effect on the bioimaging.

#### 2.4. Fluorescent supermacromolecular nanoassemblies

Fluorescent supermacromolecular nanoassemblies, such as micelles/vesicles [137–140], nanofibers [103,141–143], nanowires [144] and nanotubes [145], have been studied for bioimaging (Fig. 10). These fluorescent nanostructures were formed through assembly of small organic dye molecules [146] and/or fluorescent

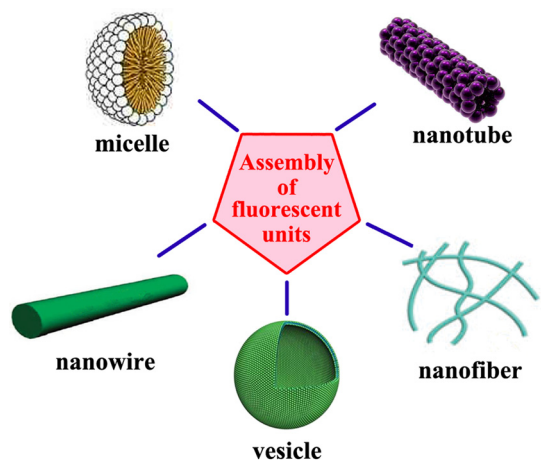


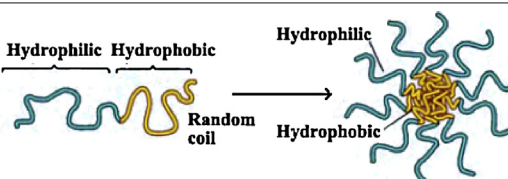
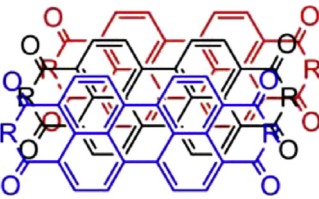
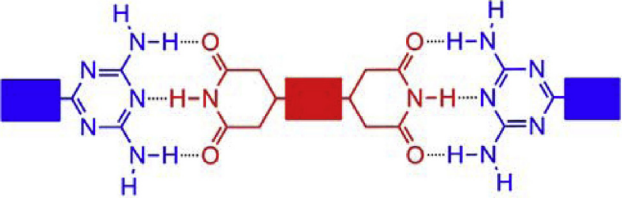
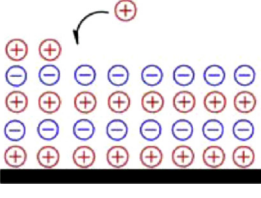
**Fig. 10.** Different supermacromolecular nano-assemblies formed by self-assembly of fluorescent units. The assemblies included micelles/vesicles [137–140], nanofibers [103,141–143], nanowires [144] and nanotubes [145].

copolymers [147,148]. The reported intermolecular interactions and the self-assembly mechanism are summarized in Table 2. As reported, the assembling could occur under certain conditions, including solvent, temperature, etc., thus the assembling chance of either small organic dye molecules or fluorescent copolymers was limited. Therefore, the experimental conditions should be accurately controlled. However, the size of FNS (usually in range of 1.5–160 nm as reported) could not be easily controlled because of the complexity of assembling process.

It is well known that fluorescent units with amphiphilic structures could self-assemble into vesicle/micelle-like aggregates, which are resulted from the intermolecular interaction within hydrophobic and hydrophilic moieties, respectively. Since copolymers could be designed to have different functions in the block sections, amphiphilic polymers are generally inclined to self-assemble into uniform structures. Therefore, fluorescent amphiphilic structures are usually designed as graft [160] or block [161,162] copolymers. For instance, Chang et al. [163] synthesized a Rhodamine B (RhB)-anchored amphiphilic poly(poly(ethylene glycol)methacrylate)-*b*-poly(glycidyl methacrylate) block copolymer (PPEGMA-*b*-PGMA/RhB), in which the inter-molecular interaction of RhB resulted in the assembled fluorescent NPs. The nanoassembly PPEGMA-*b*-PGMA/RhB was then introduced into HeLa cells and the HeLa cells exhibited good fluorescence images (Fig. 11). Li et al. [160] also reported the similar results by using comb-like graft copolymer poly((N-vinylcarbazole)-co-(4-vinylbenzyl chloride))-comb-poly(((2-dimethylamino)ethylmethacrylate)-co-(acrylic acid)) (P(NVK-co-VBC)-comb-(DMAEMA-co-AAc)) to produce self-assembled hollow vesicles with multi-walls, which even exhibited good fluorescence intensity in aqueous media. Compared with liner copolymers, self-assembly of functional star polymers provides a convenient method to construct nanoaggregates with different functionalities [164]. For example, Cheng et al. [165] successfully synthesized star polymers by using a

**Table 2**

Intermolecular interactions and the mechanism of self-assembly.

Intermolecular interaction	Mechanism of self-assembly	Refs.
Amphiphilic assemble		[149–154]
$\pi-\pi$ stack		[155,156]
Hydrogen bond		[157,158]
Electrostatic adsorption		[83,159]

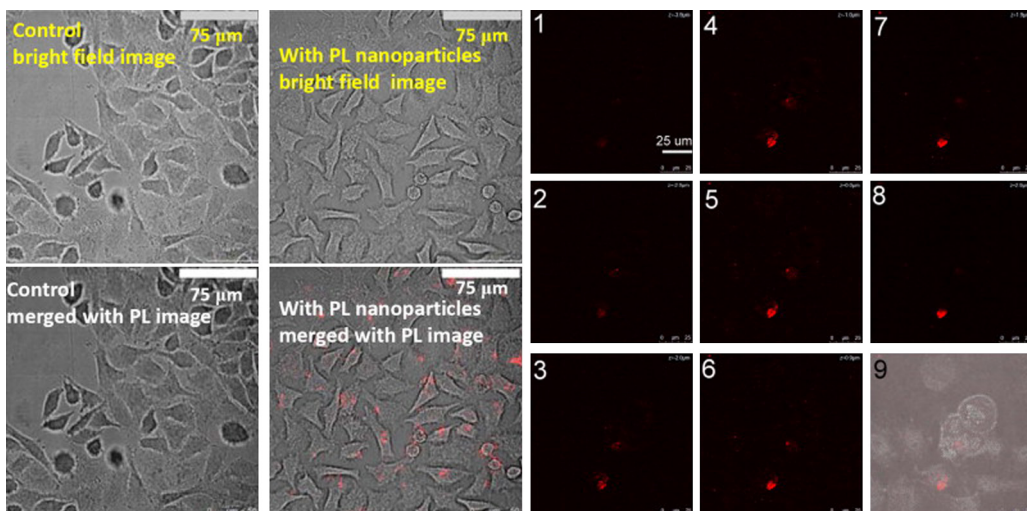


**Fig. 11.** Left: confocal images of HeLa cells incubated without (control) and with PPEGMA-*b*-PGMA/RhB nanoparticles (50 mg/mL) for 12 h. Right: z-Stack confocal images demonstrating that the nanoparticles had been taken up into the cells (images 1–8, sampling depths are increased with 1 mm every image) [163], Copyright 2012. Reproduced with permission from Elsevier Ltd.

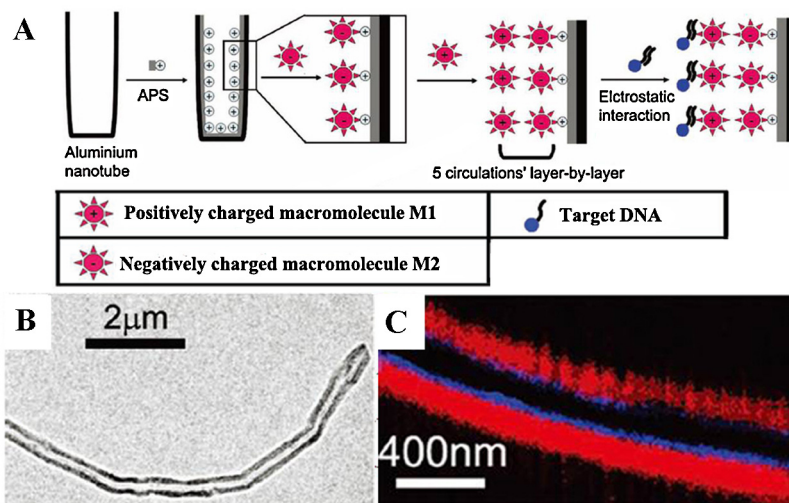


**Fig. 12.** (a) Fabrication of fluorescent nanotubes via LBL deposition of oppositely charged core-shell perylene derivatives (M1/M2); (b) TEM image and (c) fluorescent image of fluorescent nanotubes prepared via deposition of oppositely charged core-shell perylene derivatives [145]. Copyright 2011. Reproduced with permission from WILEY-VCH Verlag GmbH & Co. KGaA, Weinheim.

novel fluorescent organo-boron crosslinker with poly(*N*-isopropylacrylamide)-*b*-polystyrene (PNIPAM-*b*-PS) as linear polymer precursors, which led to the formation of large vesicle-like fluorescent aggregates; they were subsequently tailored for applications in biomaterials and biomedical systems. Since multi-functional monomers could be introduced into the assembled copolymer, the obtained FNSs by this method also exhibited great advantages in stimuli-responsive drug delivery and release systems.

Fluorescent  $\pi$ -conjugated nanostructures could form H- or J-aggregates due to the facile  $\pi$ - $\pi$  stacking. For example, Olivier et al. [166] studied the NIR fluorescent NPs formed by self-assembly of lipidic boron-dipyrromethene dyes. The resulted supramolecular assemblies could be used as important delivery vehicles for living cells in which the entering of particle could be monitored directly with fluorescence microscopy.

Since some  $\pi$ - $\pi$  interaction systems might show serious self-quenching of the fluorescent units, it is challenging to obtain highly fluorescent assemblies. The introduction of hydrogen bonding and electrostatic interaction has been shown as a potential solution to produce FNSs with high fluorescent intensity. For example, Gassensmith et al. encapsulated highly fluorescent NIR squaraine dyes inside macrocycles through hydrogen bonding between squaraine oxygen groups and macrocycle amide NH residues [167]. The resulting highly fluorescent, near-infrared complexes showed great promise in bioimaging [168]. Through layer-by-layer (LBL) assembly with the electrostatic interaction, Yin et al. applied aluminum nanotubes as templates and deposited oppositely charged core-shell perylene derivatives on them to generate novel fluorescent nanotubes (Fig. 12) [145]. These nanotubes can be used as biosensors to detect DNA in a dual-response manner.

Intermolecular multi-interactions induced assemblies have also been reported, which can drive the fluorescent units selectively to self-assemble in complicated

biological environments and form discrete complexes with well-defined structures. For example, Xu et al. [169] reported the formation of water-miscible organic J-aggregate nanoassemblies from the cooperation between  $\pi$ - $\pi$  stacking and hydrogen-bonding interactions of 1,4-dimethoxy-2,5-di [4'-(cyano)styryl]benzene (COPV). And the J-aggregated COPV nanoassemblies were highly emissive in aqueous media, which were also used as efficient two-photon fluorescent nanoprobe in bioimaging. Dual-color fluorescent nanofibers assembled in two strategies have been reported by Yin et al. [103]. They synthesized a novel water-soluble hexa-peri-hexabenzocoronenes (HBCs) derivative with peripheral functional groups (Fig. 13(a)), which facilitated a two-step assembly into nanofibers in water: (1) in the first step, the HBC derivative self-assembles via  $\pi$ - $\pi$  stacking into water soluble fibers with red fluorescence (Fig. 13(b)); (2) in the second step, the peripheral functional groups bind to the positively charged 5(6)-Fam-conjugated peptides with green fluorescence (Fig. 13(c)), leading to the formation of well-defined dual-color fibers (Fig. 13(d)). The advantage of hybrid design is to maintain the well-studied fluorescence of HBC chromophores, which allows the direct monitoring of the assembly process with fluorescence microscopy. This was the first report on fiber-forming HBC derivatives as a template for further functionalization of biomolecules.

## 2.5. Aggregation-induced emission fluorophores

Generally, most organic fluorescent materials mentioned in preceding perform well for bioimaging in solution state. However, fluorescence quenching or decrease in luminous efficiency occurs when their solution concentrations are increased or they are aggregated in the solid state. The phenomenon is identified as aggregation-caused quenching (ACQ). The compacted aggregation may lead to the radiationless energy conversion or the formation of detrimental species as excimers, resulting in fluorescence

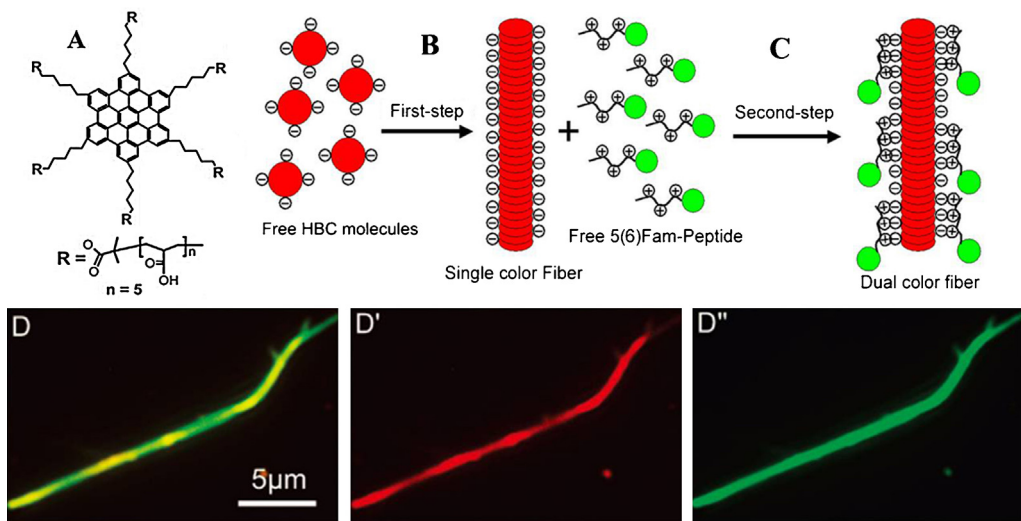


**Fig. 13.** (a) Structure of HBCs; (b)  $\pi-\pi$  stacking of negatively charged HBCs into red fluorescent fibers; (c) positively charged 5(6)-Fam-conjugated peptides with green fluorescence bound to the negatively charged red fiber through electrostatic interactions, resulting in the formation of a dual-color fiber for double-fluorescence imaging; (d) fluorescence image of the formed dual-color fiber in different channels [103]. Copyright 2009. Adapted with permission from the American Chemical Society.

quenching [170]. Thus, the ACQ effect limits the bioapplication of such fluorescent materials as labeling or imaging agents.

In 2001, Tang et al. first discovered novel fluorescent materials (1-methyl-1,2,3,4,5-pentaphenylsilole) that could generate aggregation-induced emission (AIE) [171] and effectively avoided the obstacle from ACQ. These FNSs showed quite low FQY (0.03–0.3%) in solution, while high FQY (14–50%) in aggregate states. They offered a new fabrication of solid fluorescent materials with high FQY [172–174]. Up to present, a large number of new AIE luminogens have been designed and synthesized, such as silole, tetraphenylethene (TPE), triphenylamine (TPA), 9,10-distyrylanthracene (DSA), 1,4-distyrylbenzene (DSB) and their derivatives, as listed in Table 3.

In addition, these AIE fluorophores were usually further modified to improve their performance as imaging agents, *i.e.*, biocompatibility, brightness, permeability, retention effect, *etc.* For example, Qin et al. [185] had attached TPE units as terminals to 2-(2,6-bis((E)-4-(diphenylamino)styryl)-4H-pyran-4-ylidene)malononitrile (TPA-DCM) (Fig. 14), and the resulted TPE-TPA-DCM showed a novel phenomenon of AIE. Based on this result, bovine serum albumin (BSA) had been used as the polymer matrix to fabricate BSA-formulated TPE-TPA-DCM NPs with efficient far-red/near-infrared (FR/NIR) fluorescence and low cytotoxicity (Fig. 14). Their *in vitro* and *in vivo* FR/NIR bioimaging were successfully demonstrated with MCF-7 breast-cancer cells and a murine hepatoma-22 (H22)-tumor-bearing mouse model, respectively (Fig. 14).

Generally, the abnormal emissive feature of AIE fluorophores is different from “conventional” luminophores. AIE fluorophores show great potential in bio-fluorescence system since aggregation occurs in many biological processes. Because the AIE effect allows the use of highly concentrated fluorogen solution as well as their nanoaggregates

in applications of biosensor, AIE fluorogens are supposed to become practical tools in biological world very soon.

### 3. Inorganic fluorescent nanostructures

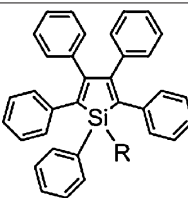
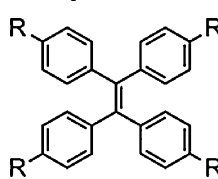
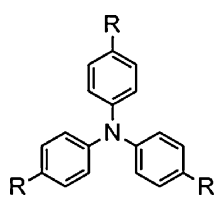
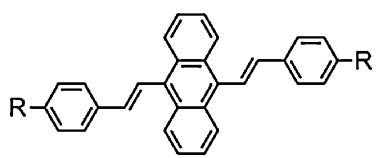
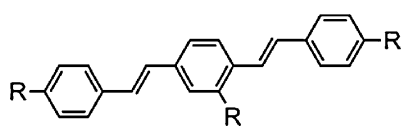
Inorganic FNSs are usually nanoclusters (NCs) or NPs with great potential advantages in bioimaging because of their interesting self-fluorescent properties. It was well known that, with very few exceptions, fluorescent lifetimes of organic dyes are too short (1–10 ns) for efficient temporal discrimination of short-lived fluorescence interference from scattered excitation light. Comparatively, inorganic FNSs have longer lifetimes (typically five to hundreds of nanoseconds) [192], which makes them as better candidates for bioimaging. According to their compositions, inorganic FNSs could be divided into various classifications, such as quantum dots, silicon nanoparticles, fluorescent metallic NPs and complexed inorganic FNSs.

#### 3.1. Quantum dots

Quantum dots (QD), tiny semiconductor crystals, are regarded as one of the most important building blocks in modern photonics. The bright and photostable fluorescence of QD (FQY = 0.1–0.8 (visible), 0.2–0.7 (NIR)) has made it an excellent optically selective marker in bioimaging [193–195]. Compared with organic dyes, large Stock shift of QDs allows them to avoid the overlap between emission spectrum and excitation spectrum effectively, which increases the detection sensitivity of fluorescence signal. To date, the synthesis of QDs with controlled emission and absorption properties has already been a mature technique by adequately tailoring their sizes (1–10 nm) [196]. Therefore, through technically controlling the sizes and chemical compositions of QDs, their emission spectra could cover the whole visible region (Fig. 15). Furthermore, QDs provide a broad excitation spectrum and a narrow

**Table 3**

The most reported fluorescent materials with aggregation-induced emission (AIE) phenomenon.

AIE fluorophores	General structural formula	Refs.
Silole		[175–179]
TPE		[180–184]
TPA		[185,186]
DSA		[187–189]
DSB		[190,191]

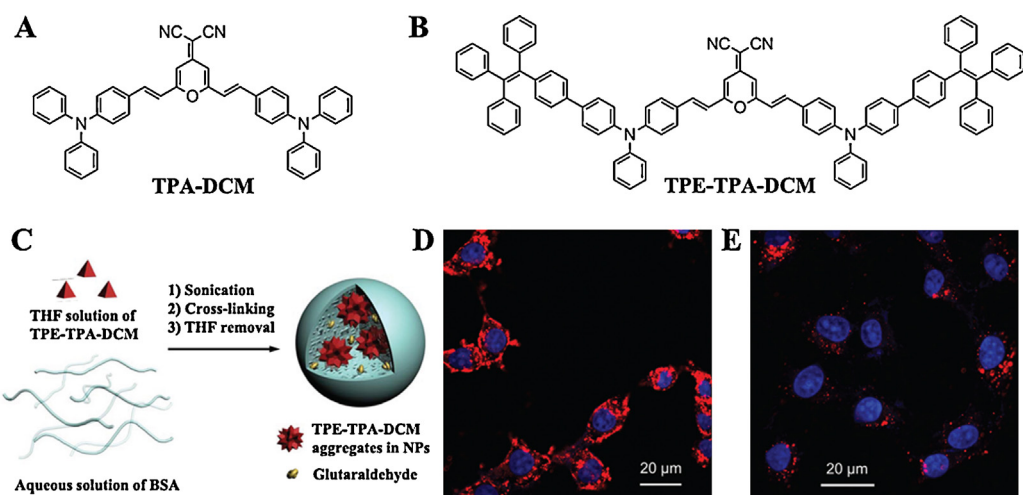


**Fig. 14.** Chemical structures of (a) TPA-DCM and (b) TPE-TPA-DCM. (c) Schematic illustration of the fabrication of BSA NPs loaded with TPE-TPA-DCM. (d and e) CLSM images of MCF-7 breast cancer cells after incubation with (d) fluorogen-loaded BSA NPs (with a fluorogen loading of 0.86%) and (e) bare TPE-TPA-DCM NPs for 2 h at 37 °C. [TPE-TPA-DCM] =  $0.4 \times 10^{-6}$  M [185]. Copyright 2012. Reproduced with permission from WILEY-VCH Verlag GmbH & Co. KGaA, Weinheim.

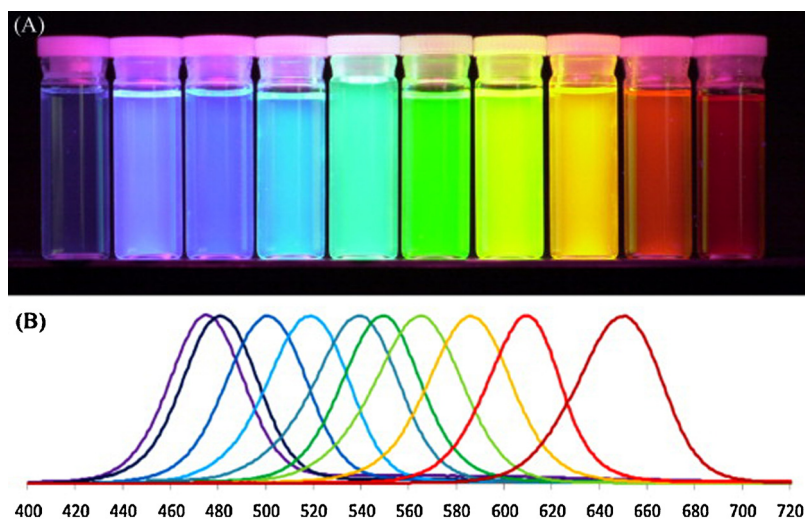


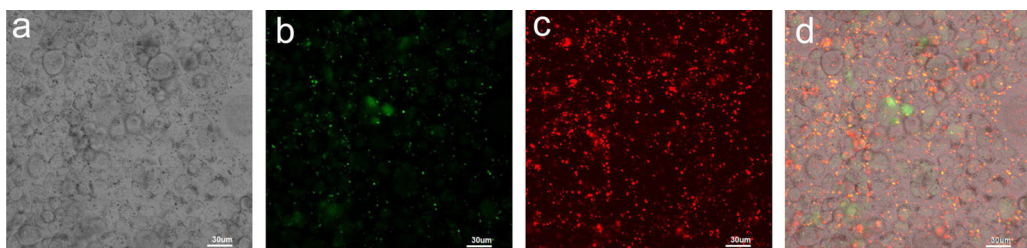
**Fig. 15.** (a) Colloidal suspension of quantum dots with different sizes viewed under long-wave ultraviolet illumination; (b) narrow emission spectra of related quantum dots with different sizes [197]. Copyright 2019. Reproduced with permission from Elsevier Ltd.

emission spectrum, so QDs with different sizes could be detected by utilizing the same excitation light source. This unique feature makes the multi-color labeling possible and greatly promotes their application in bioimaging.

Most of the highly fluorescent QDs for bioimaging contain toxic elements (Cd, Pb, Se, Te, etc.) [198–200]. Prasad and his co-workers [201] have done excellent work to summarize toxicities of different QDs in varied *in vivo* systems. Although numerous studies on low-toxic/non-toxic QDs have been reported recently, many scientists are still working on QDs with chemical stability and lower cytotoxicity [202]. For example, Peng et al. [203] reported the synthesis of CdSe QDs using CdO as Cd precursor to replace the toxic CdMe<sub>2</sub>, so QDs could be prepared in a safer and more economical way. Recently, effort has been made in developing methods to prepare non-toxic QDs. Deng et al. [204] synthesized high-quality CuInS<sub>2</sub>/ZnS (CIS/ZnS) QDs without toxic heavy metals, which avoided the intrinsic toxicity of well-developed II–VI and other semiconductor QDs (Cd, Pb, Se, Te, etc.) that was the major obstacle to their clinical applications. And they also demonstrated the versatility of the biocompatible CIS/ZnS QDs in multi-color bioimaging. Fig. 16 clearly shows their high labeling

specificities on folic acid (FA) receptor expressing Bel-7402 cells compared with that of fluorescein FITC (the green and red fluorescence signals are attributed to FITC and the encapsulated QDs, respectively). Such a toxicity study has also been done both in cellular level and in small animals. For example, Ye et al. [205] reported a pilot study in which rhesus macaques injected with phospholipid micelle-encapsulated CdSe/CdS/ZnS quantum dots did not exhibit evidence of toxicity. Blood and biochemical markers remained within normal ranges after treatment, and histology of major organs after 90 days had no abnormalities. These results indicated that acute toxicity of these QDs *in vivo* could be minimal.

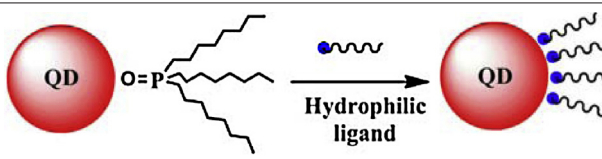
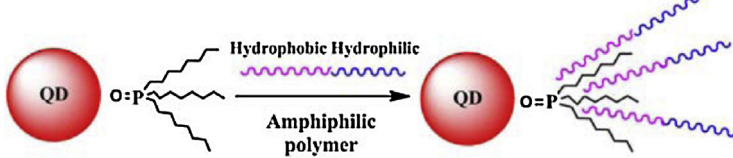
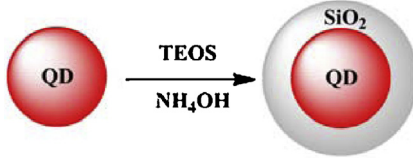
The major problems of QDs in bioimaging are their toxicity, low stability, poor solubility, poor biocompatibility and blinking effect (intermittence in emission). In order to solve these problems while maintaining their advantages in bioimaging, several strategies including surface passivation and functionalization (ligand exchange, polymer incorporated, etc.) were explored [206], as summarized in Table 4. Additionally, many reported synthetic procedure lead directly to QDs covered with polymers and small molecules, thus the process of surface passivation



**Fig. 16.** Optical microscopy of live FA receptor-positive Bel-7402 cells incubated with FITC-labeled and QDs-loaded micelles: (a) differential interference contrast (DIC), (b) fluorescein, (c) 625 nm emitting QDs-loaded micelles, (d) the merged image of the fluorescence images and DIC image.  $\lambda_{ex} = 488$  nm; scale bar: 30  $\mu$ m [204]. Copyright 2012. Reproduced with permission from the American Chemical Society.

**Table 4**

Strategies in surface passivation and functionalization of QDs.

Strategies in surface passivation and functionalization of QDs	Refs.
Hydrophilic ligand exchange	 [210–213]
Amphiphilic polymer/small molecule interaction	 [214–217]
Additional inorganic shells	 [218–221]

could be omitted [207,208]. Currently, potential applications of QDs in non-invasive bioimaging emerge as superior alternatives in bioimaging and their applications in both basic and applied biology are expanding. For example, Feugang et al. [209] reported bioluminescent resonance energy transfer-conjugated QDs (BRET-QDs) and their applications in real-time *in situ* fluorescence imaging of spermatozoa. Since spermatozoa can be incorporated with BRET-QD without affecting their motility and capacity to interact with oocytes when they are used at an appropriate ratio, the non-invasive bioimaging can be realized. The blinking effect of QDs (as well as metal, carbon, and silicon based FNSs) has limited their applicability to single molecule analysis [192], which will not be discussed in detail here in order to focus on their bioimaging applications.

### 3.2. Silicon nanoparticles

Over the last few years silicon nanoparticles (SiNPs) have attracted many attention due to their exceptional optical properties [222–224], such as size-dependent tunable light emission, high brightness ( $FQY = 12\text{--}76\%$ ), great stability against photo-bleaching compared with organic dye molecules [225–227], and low inherent toxicity compared with the heavy elements of above-mentioned semiconductor QDs [228]. However, SiNPs usually possess poor aqueous dispersibility due to the surface-covered hydrophobic functional groups (e.g., Si–H bond) [229]. Substantial progress has been made in recent years in producing hydrophilic SiNPs [230]. For example, Zhong et al. developed a one-pot bottom-up strategy for the facile, rapid, and large-scale synthesis of SiNPs in water [231]. Significantly, the as-prepared SiNPs had excellent aqueous dispersibility, ultrahigh photo- and pH-stability, strong fluorescence, and excellent biocompatibility. And cellular experiments showed that the SiNPs were superbly suitable for long-term and real-time cellular imaging.

Currently, SiNPs have been adopted as a nontoxic alternative to toxic QDs due to their several advantages [232,233]: (1) the flexible surface chemistry, which allows them to be conjugated with biomacromolecules; (2) SiNPs exhibit NIR emission when their sizes are small, allowing deep-tissue imaging; (3) highly photostability, useful for long-term imaging; (4) tunable fluorescence with altering sizes and capping groups.

### 3.3. Fluorescent metallic nanoclusters

A fluorescent metallic nanocluster (NC), composed of a few to roughly a hundred atoms, has many attractive features, including ultrasmall size (less than 2 nm), good biocompatibility, good photostability, large Stokes shift (more than 100 nm) and high emission rate ( $FQY = 0.01\text{--}0.1\%$ , bare NCs), which make it a promising candidate for fluorescent bioimaging [234–236]. Since the 1990s, metallic NCs with self-fluorescent properties have been investigated widely [237]. However, no general mechanism has been currently known to explain the emission from any metal NC. Recent studies suggested that there might be two major sources for the fluorescence of metal NCs [238]: the metal core with its intrinsic quantization effects and the particle surface that is dependent on the chemical interaction between the metal core and the surface ligand. Therefore, the emission wavelength (typically in 400–700 nm) of metal NCs may be varied with size, coating ligand and/or even synthetic method [239]. However, the theory of size-dependent optical properties may not be suitable for all metallic NCs. In pure metallic NCs, aggregation can occur when two NCs are very close, resulting in metallic dimmers or assemblies [240]. Then their surface plasmon resonances will be coupled together, and the local electric field in the junction region will be largely enhanced [241], which is identified as surface-enhanced Raman scattering. Thus, enhanced two-photon luminescence of the

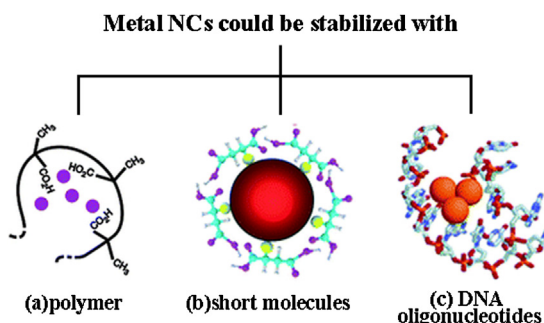


**Fig. 17.** Different strategies to functionalize metal NCs: (a) stabilization with polymer; (b) stabilization with short molecules; (c) stabilization with DNA oligonucleotides [238]. Copyright 2011. Adapted with permission from Elsevier Ltd.

metallic NCs would turn to be independent with the size or geometry.

Among the reported fluorescent metallic NCs, Au and Ag NCs gained most attention because of their monodispersity, brightness, photostability and potential optical-imaging applications [236,242]. There were many reports on the application of fluorescent Au and Ag NCs in bioimaging in the past few years [243–245]. Since Au and Ag NCs show size-dependent fluorescence, this controllable optical property offers them great advantages in bioimaging application [246,247]. In literatures, Au and Ag NCs were usually capped with different ligands during their syntheses in order to improve their water solubility and stability (Fig. 17) [238,248–251]. Further functionalization of Au and Ag NCs could be realized with different functional ligands as their capping agents, in which thiol-containing organic linkers were mostly used owing to the strong interaction between thiol and Au/Ag [252–254], and recently some zwitterionic functional ligands had also been reported [255]. Moreover, the usage of proteins as green reducing and stabilizing agents of these NCs is an additional advantageous strategy for target-specific cell imaging [242]. For example, Liu et al. [256] performed insulin-directed synthesis of fluorescent Au NCs as bioimaging agents, which had strong red fluorescence, excellent biocompatibility and preservation of natural insulin bioactivity to lower blood-glucose level. And, in C<sub>2</sub>C<sub>12</sub>, a mouse myoblast cell line, the synthesized insulin-Au NCs specifically stained the cytoplasm (Fig. 18). Similarly, Guével et al. [257] synthesized

Ag NCs coated with glutathione and demonstrated their uptaking by the epithelial lung cancer, which indicated a high potential in biolabeling and bioimaging.

Apart from above-mentioned spherical morphology, extensive studies on metallic NCs with varied geometries have been reported recently, such as nanorod [258,259], nanoprisms [260,261], nanocages [262,263], and nanocubes [264,265]. Since these metallic NCs could generate visible or NIR fluorescence, their bioimaging application have also been investigated with increasing interests. For example, Wang et al. has reported a facile route to prepare radioluminescent Au nanocages without additional radiolabeling or dye conjugation [262]. The AuNCs were shown to emit luminescence with continuous wavelengths in the visible and NIR regions, enabling luminescence imaging of the whole mice *in vivo*, as well as their organs *ex vivo* for direct gamma counting. Due to their increased specific surface area, these metallic NCs showed excellent performance in many other application rather than bioimaging [266], such as photo-thermal sensors, drug delivery, and cancer diagnosis. The bioimaging performance of metallic NCs with varied geometries will not be discussed in detail here. In addition, toxicity of such metallic NCs in bioimaging have also been analyzed, which was related to the particle size, concentration, and surface modification [267]. It was believed that bare metallic NCs and their aggregates had hazardous effect to human bodies. Thus, surface modification of NCs has been paid more attention for their bioimaging during these years, which will be discussed in the following.

### 3.4. Complexed inorganic fluorescent nanostructures

#### 3.4.1. Upconversion nanoparticles

Traditionally, when fluorescent materials are exposed to incident light irradiation (typically ultraviolet (UV) light or X-ray) at specific wavelength, they emit low-energy photons (usually visible or NIR light) (Fig. 19). Recently, another type of FNSs with different luminous mechanism, *i.e.*, upconversion nanoparticles (UCNPs), has been studied. These FNSs could emit high-energy photons under NIR excitation [268–271]. The phenomenon of “upconversion” (UC) was defined as a nonlinear optical process in which the sequential absorption of two or more photons leads to the emission of a single photon at a shorter wavelength [272].

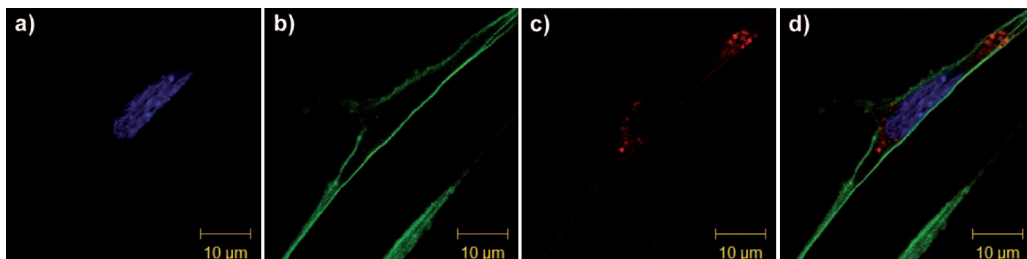


**Fig. 18.** Microscopic observation of the uptaking of insulin-Au NCs by differentiated C<sub>2</sub>C<sub>12</sub> myoblasts after 2 h: (a) Cell nucleus stained with 4',6-diamidino-2-phenylindole (DAPI, blue); (b) actin fiber stained with Alexa Fluor 488 phalloidin to confirm the cell boundary (green); (c) insulin-Au NCs with red luminescence in the cytoplasm; (d) fluorescence image overlay of the three images [256]. Copyright 2011. (For interpretation of the references to color in this figure legend, the reader is referred to the web version of the article.) Reproduced with permission from WILEY-VCH Verlag GmbH & Co. KGaA, Weinheim.

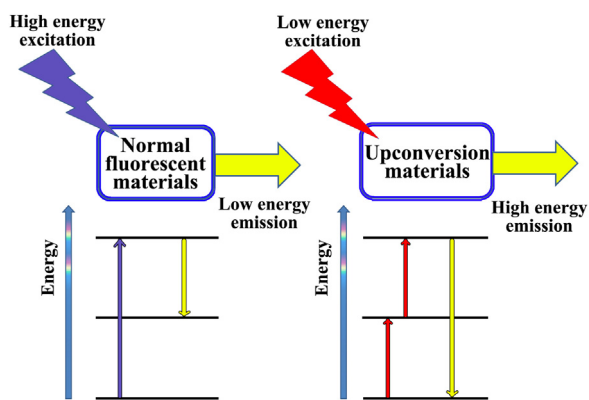


**Fig. 19.** Energy level diagram of the emission processes of normal fluorescent materials and upconversion materials.

Since the discovery of UC process in the 1960s [273], UCNPs have shown great advantages in bioimaging [274–276]. The reasons are the following: (1) UCNPs minimize the optical damage to cell tissues; (2) NIR light irradiation exhibits high tissue penetration; (3) the emission locates in visible or NIR region, so the interference of background radiation can be effectively avoided; (4) UCNPs show excellent photostability and low toxicity as bioimaging agents.

The reported UCNPs are usually a rare earth(RE)-doped inorganic host matrix. The host matrix is required to have low lattice photon energies, most of those reported as are oxide, halide, sulfide or oxysulfide [277,278]. The doping RE ions (lanthanide) play roles as a sensitizer ( $\text{Yb}^{3+}$ ) and

an activator ( $\text{Er}^{3+}$ ,  $\text{Ho}^{3+}$ ,  $\text{Tm}^{3+}$ ) [279,280]. In addition to the synthesis of new RE-doped UCNPs, many groups studied the surface modification of UCNPs to obtain better water dispersibility and biocompatibility for bioimaging. For example, Bogdan et al. reported the functionalization of ligand-free UCNPs with heparin and basic fibroblast growth factor (bFGF) [281]. These heparin-bFGF functionalized UCNPs showed specific binding capabilities to *HeLa* cell membranes, which resulted in high-contrast images of *HeLa* cells (Fig. 20). In addition, these fluorescent materials offered feasibility for bioimaging not only in the visible but also in the NIR region (first and second biological window) [276,282]. Nyk et al. [283] synthesized aqueous dispersible fluoride ( $\text{NaYF}_4$ ) nanocrystals (20–30 nm size) that were co-doped with the rare earth ions ( $\text{Tm}^{3+}$  and  $\text{Yb}^{3+}$ ), showing NIR-to-NIR ( $\lambda_{\text{em}} = 800 \text{ nm}$ ,  $\lambda_{\text{ex}} = 975 \text{ nm}$ ) upconversion for *in vitro* and *in vivo* photoluminescence imaging. This NIR-to-NIR upconversion process provides deeper light penetration into biological specimen and results in high contrast optical imaging due to the absence of an auto-fluorescence background and decreased light scattering.

However, RE-doped UCNPs have their shortcomings, such as the low absorption cross-section of  $\text{Yb}^{3+}$  and the low upconversion FQY (~0.5%) [284]. These problems inspire researchers to explore new types of UCNPs without RE ions. Liu et al. [285] successfully synthesized the water-soluble UCNPs based on triplet-triplet annihilation (TTA) by co-loading sensitizer (octaethylporphyrin Pd complex) and annihilator (9,10-diphenylanthracene) onto silica nanoparticles, whose upconversion FQY could be as high as 4.5% in aqueous solution (Fig. 21). And those

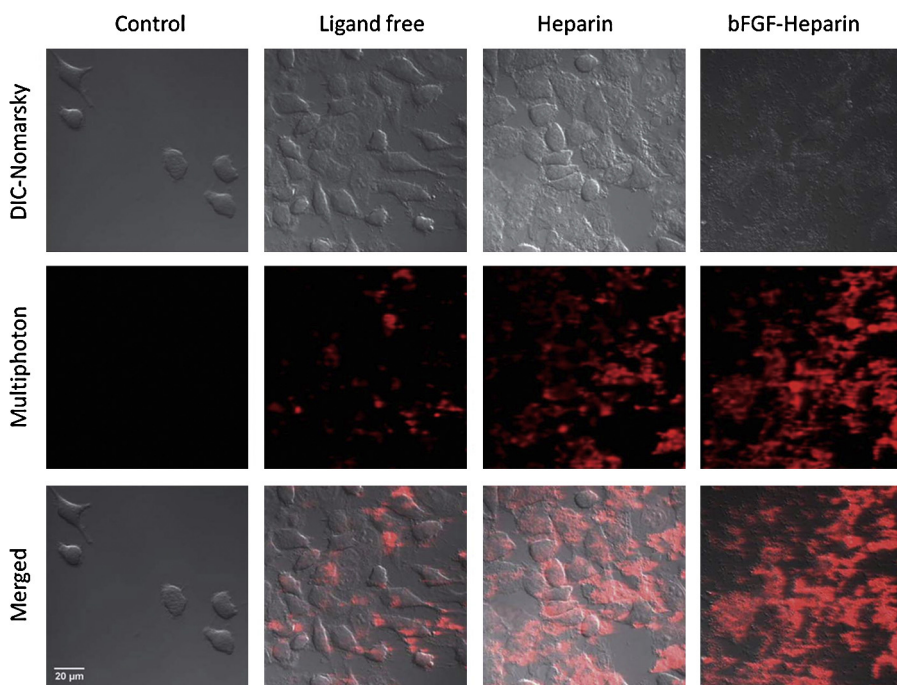


**Fig. 20.** Optical transmission images (top row), fluorescence images (middle row), and the overlay images (bottom row) of a group of *HeLa* cancer cells which were incubated at 37 °C with a phosphate buffered solution (PBS) (control) or a PBS containing 5 mg/mL of ligand-free heparin and bFGF-heparin coated UCNPs. Scale bar: 20  $\mu\text{m}$  [281]. Copyright 2012. Reproduced with permission from the Royal Society of Chemistry.

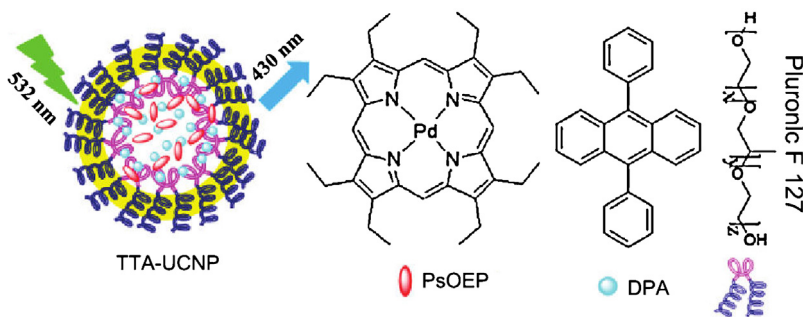


**Fig. 21.** Schematic illustration of upconversion luminescence of TTA-UCNPs, and chemical structures of PdOEP, DPA, and F127 [285]. Copyright 2012. Adapted with permission from the American Chemical Society.

TTA-based UCNPs showed low cytotoxicity and were successfully applied in the *in vivo* imaging of lymph node in living mouse with an excellent signal-to-noise ratio.

Compared with those of down-conversion FNSs, applications of UNCPs as probes in high-contrast and low-power-excited *in vivo* bioimaging (in both visible and NIR region) may expand the arsenal of currently available fluorescent bioimaging both *in vitro* and *in vivo*.

#### 3.4.2. Inorganic core/shell fluorescent nanoparticles

Even the inorganic FNSs showed great advantages in bio-application, they were often used after further surface functionalization rather than being used directly. Modified silica surfaces are preferred to achieve the desirable features of hydrophilicity, biocompatibility and low toxicity, silica surface. Zhang et al. [286] successfully synthesized silica-wrapped gold nanocluster ( $\text{Au@SiO}_2$ ) with good water solubility, exceptional biocompatibility, favorable surface properties and excellent fluorescence properties. After covalently modified with folic acid (FA),  $\text{Au@SiO}_2$  nanocomposite was exceptionally suitable for cellular imaging by effectively recognizing the expressed FA receptors on HeLa cell's surface (Fig. 22). Since similar work on both silica-coated QDs and metallic NCs have already been widely reviewed, more attention would be preferred to core/shell structural UCNPs. An increasing literature has been reported on the bioimaging of silica-coated UCNPs

due to their strong NIR-to-visible upconversion fluorescence, attracting substantial interest in the development of various types of inorganic shell to give UCNPs better biocompatibility [287,288]. Several aspects should be taken into consideration when choosing the epitaxial shell materials, *i.e.*, the lattice mismatch with inner core, optical transparency, crystallizability and stability. For example, Chen et al. [280] developed heteroepitaxial growth of a biocompatible  $\text{CaF}_2$  shell over UCNPs ( $\alpha\text{-NaYbF}_4:\text{Tm}^{3+}$ ) to suppress surface quenching effects, resulting in core/shell ( $\alpha\text{-NaYbF}_4:\text{Tm}^{3+}$ )/ $\text{CaF}_2$  NPs that exhibit highly efficient  $\text{NIR}_{\text{in}}\text{-NIR}_{\text{out}}$  UC for high contrast and deep bioimaging.

Some studies have used silica as supporting matrix as well as coating materials [289]. For example, Jun et al. [290] synthesized highly bright QD-embedded nanoprobes ( $\text{Si@QDs@Si NPs}$ ) by embedding a large number of hydrophobic QDs onto the surface of hydrophilic silica NPs, which were then covered with a silica layer (Fig. 23(a)). These  $\text{Si@QDs@Si NPs}$  exhibited approximately 200-times stronger fluorescence than single QDs and also showed high brightness and biocompatibility for effective bioimaging of cells in mouse skin (Fig. 23(b) and (c)).

Moreover, such surface functionalization would also be realized by applying polymer network or organic biological molecules as protecting agents or scaffolds to ensure better bio-compatibility. Therefore, organic/inorganic hybrid FNSs have been rapidly developed recently.

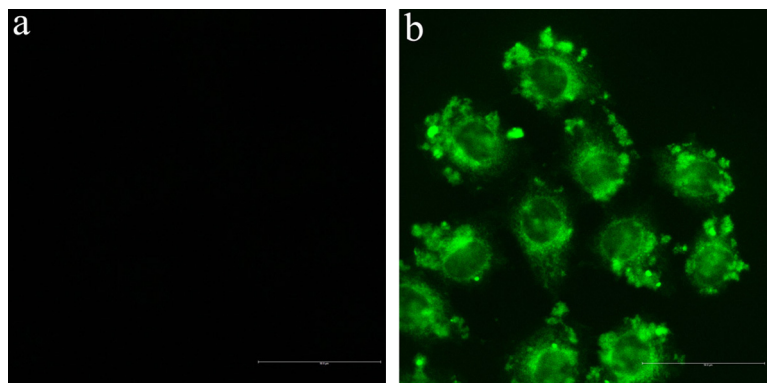


**Fig. 22.** Confocal fluorescence images of HeLa cells treated with the following nanoparticles: (a) 11-MUA Au-NCs@ $\text{SiO}_2$  in the HeLa cells incubated at 37 °C; (b) 11-MUA Au-NCs@ $\text{SiO}_2$ -FA in the HeLa cells incubated at 37 °C. Scale bar: 50  $\mu\text{m}$  [286]. Copyright 2011. Adapted with permission from Elsevier Ltd.

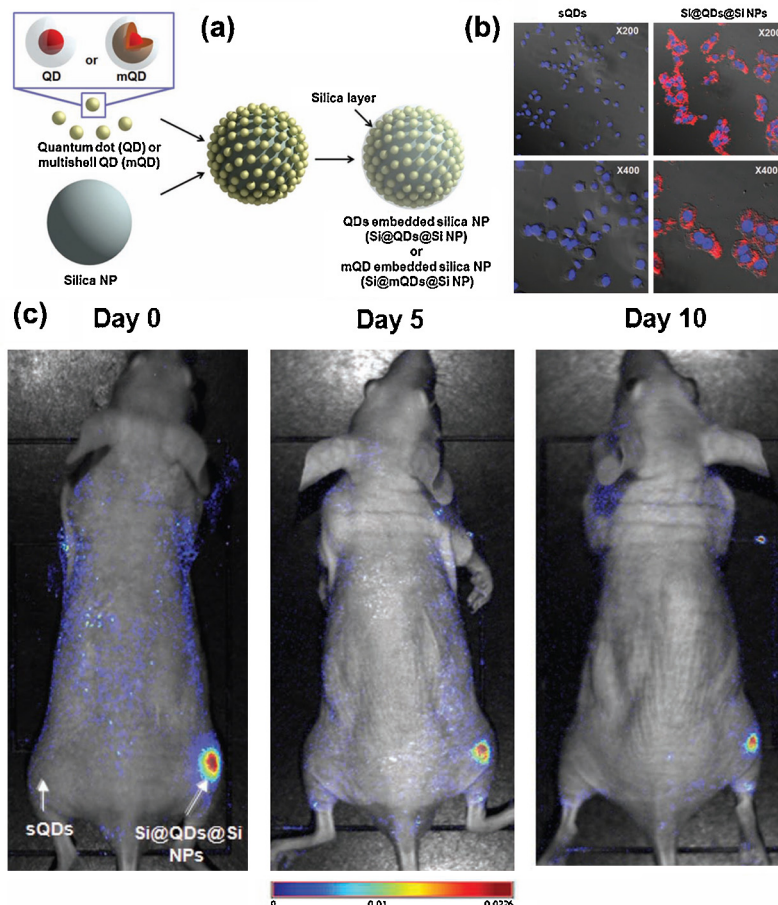


**Fig. 23.** (a) Synthesis of silica-coated QD or mQD-embedded silica NPs, in which core–shell QDs (QDs) and core–multishell QDs (mQDs) were immobilized to thiol-modified silica NPs; Si@QDs@Si NPs and Si@mQDs@Si NPs were then prepared by silica–shell encapsulation; (b) fluorescence images of QD- and Si@QDs@Si-NP-uptaken cells (red color: QD; blue color: DAPI); (c) Maestro *in vivo* fluorescence image of sQD-labeled (left leg) and Si@QDs@Si-NP-labeled (right leg) cell-transplanted mouse [290]. Copyright 2012. (For interpretation of the references to color in this figure legend, the reader is referred to the web version of the article.)

Reproduced with permission from WILEY-VCH Verlag GmbH & Co. KGaA, Weinheim.

#### 4. Organic/inorganic hybrid fluorescent nanostructures

With rational design, combining multiple constituents into a single nanoobject will not only bridge the unique properties of individual sections, but also improve conventional sensing, imaging, and therapeutic efficacies. To improve the application in bioimaging, FNSs are usually designed as organic/inorganic hybrid compositions. The core and shell segments alternately contributed to the desired fluorescent properties or acted as protecting agents of matrix or scaffold, which thus offers better functionalization and biocompatibility.

##### 4.1. Inorganic@organic hybrid fluorescent nanostructures

Inorganic@organic hybrid FNSs are mostly consisted of fluorescent inorganic composition embedded inside an organic matrix. According to literatures, the organic shell could be in the following three types: (1) polymeric

network [215,291–294], which was usually induced via ATRP followed by the attachment of an ATRP initiating group to the surface. For example, Wu et al. [295] used nonlinear PEG-based nanogel network chains as a three-dimensional scaffold to protect ZnO QDs, which was followed by appropriate growth of metallic Au, and the resulted hybrid NPs performed well in lighting up B16F10 cells; (2) self-assembled micelles [296,297], in which fluorescent inorganic cores were mostly embedded physically. For example, Hu et al. [298] demonstrated the usage of PEGylated phospholipid micelles to encapsulate NIR emitting ultra-small lead sulfide (PbS) QDs to label RAW264.7 macrophage cells (Fig. 24); (3) dendrimers [299–302], which provided cavities to trap inorganic fluorophores. For example, Alcalá et al. [303,304] created a dendrimer complex by substituting thirty-two naphthalimide fluorophores on the surface of the dendrimer and incorporating eight europium cations within the branches. The resulting hybrids exhibited preferential accumulation within liver tumors and were suitable for fluorescence imaging.

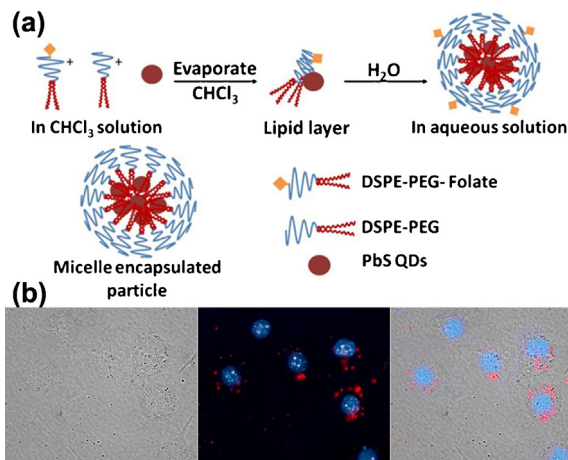


**Fig. 24.** (a) Schematic illustration of the PEGylated phospholipid micelle encapsulated PbS QDs; (b) RAW264.7 macrophages labeled with micelle-encapsulated PbS QDs (red) and the cell nucleus stained with Hoechst 33342 (blue) [298]. Copyright 2012. (For interpretation of the references to color in this figure legend, the reader is referred to the web version of the article.)

Reproduced with permission from Iivyspring International Publisher.

By introducing the organic shell, the sizes would be slightly increased compared with that of the original bare inorganic fluorescent NPs. The organic shell, serving as the protecting agent, effectively avoids the photobleaching of the inner fluorescent inorganic core, thus resulting in the improvement of the stability. In addition, because of the modification with polymeric cover, it is feasible to realize the functionalization of the composite FNSs, rendering

those features of hydrophilicity, biocompatibility, specificity, environmental stimuli responsive, etc.

In addition, these FNSs could be organic chromophores-decorated inorganic nanoparticles. The inorganic core served as supporting materials and the organic portion was the fluorescent source [305]. For instance, Ma et al. [306] reported the one-pot synthesis of PEGylated mesoporous silica nanoparticles which could be labeled with NIR dye Cy5.5. The produced FNSs showed great potential in bioimaging. The supporting inorganic core determined the sizes of the composites (15–200 nm) [307], which would not change much after coated with organic chromophores [308]. However, achieving high stability was a challenge when the exposed chromophores were increased. Meanwhile, these FNSs could be designed to have properties other than fluorescence by using different inorganic cores, e.g., magnetism [309–311]. For example, Lu et al. [312] synthesized water-soluble P(PEGMA)-grafted Fe<sub>3</sub>O<sub>4</sub> nanoparticles via ATRP method, and NH<sub>2</sub> groups were introduced through a facile post-ATRP modification. Fluorescent magnetic nanoparticles (MNPs) were then obtained by attaching fluorescein FITC covalently to the NH<sub>2</sub> groups. Such FITC-MNPs can be efficiently taken up by breast cancer cells (Fig. 25). These results indicate that FITC-MNPs with both fluorescence and magnetic functionalities have great potential in bioimaging.

#### 4.2. Organic@inorganic hybrid fluorescent nanostructures

In organic@inorganic hybrid FNSs, fluorescent inorganic compositions were usually covalently attached onto the

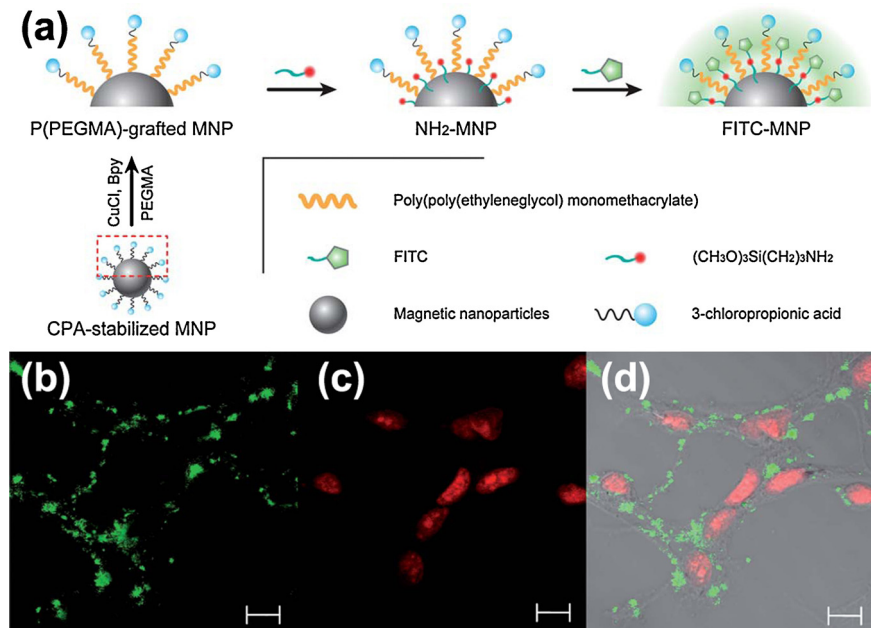


**Fig. 25.** (a) Preparation route of NH<sub>2</sub>-MNPs and FITC-MNPs from P(PEGMA)-MNPs by ATRP modification. (b–d) Confocal microscopic images of MD-MBA-231 cells after 24 h incubation with FITC-MNPs at 37 °C and further staining with PI (red). The uptake of the FITC-MNPs (green) in the MD-MBA-231 cells was visualized by overlaying the images obtained by the FITC filter and the PI filter ((b) image from FITC channel; (c) image from PI channel; (d) image from combined PI channel, FITC channel and phase contrast). Figure scale bar: 10 mm [312]. Copyright 2012. (For interpretation of the references to color in this figure legend, the reader is referred to the web version of the article.)

Adapted with permission from the Royal Society of Chemistry.

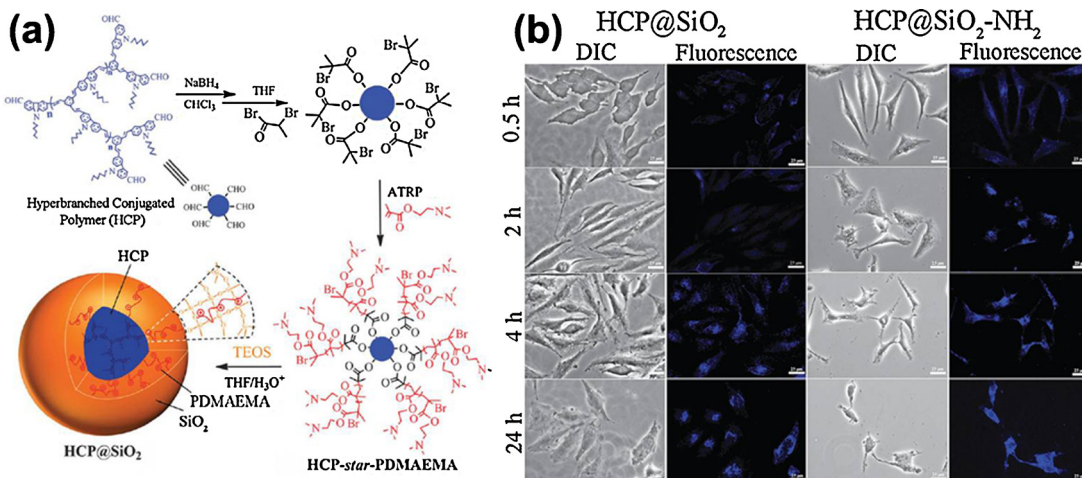


**Fig. 26.** (a) Preparation route of core–shell HCP@SiO<sub>2</sub> nanoparticles from unimolecular HCP-star-PDMAEMA; (b) fluorescence microscope images of HeLa cells incubated with HCP@SiO<sub>2</sub> and HCP@SiO<sub>2</sub>-NH<sub>2</sub>, respectively, at different time intervals (0.5 h, 2 h, 4 h, 24 h). Compared with that of HCP@SiO<sub>2</sub>, the fluorescent imaging of HCP@SiO<sub>2</sub>-NH<sub>2</sub> is brighter after a short incubation time. Scale bar: 25 μm [320]. Copyright 2012. Adapted with permission from the Royal Society of Chemistry.

surface of organic nanoparticles. For example, Yuan et al. [313] designed a QDs-labeled PAMAM G4 derivative vector for target imaging and nucleic acid delivering. This fluorescent complex dendrimer would be useful to introduce nucleic acids or drugs into cells through a receptor-targeted mechanism because significant knockdown of expression was observed. Wang et al. [314] developed a facile strategy to synthesize Fe<sub>3</sub>O<sub>4</sub>@P(St/MAA)@Chitosan@Au NPs. The obtained multifunctional NPs had a low hemolyticity as contrast agents in magnetic resonance imaging and dark field imaging.

In order to improve the stability, biocompatibility and low toxicity, sol–gel derived silica was reported as an excellent host material for creating fluorescent NPs with the covalently attached organic chromophores [315–319]. In this procedure, the organic chromophores should be functionalized via terminal siliconization first, and then their sol–gel reactions with siloxanes were carried out to produce a silica shell. For example, Qiu et al. [320] used a unimolecular fluorescent hyperbranched conjugated polymer (HCP-star-PDMAEMA) as soft template and isolated them with a silica shell to fabricate highly fluorescent core–shell hybrid NPs HCP@SiO<sub>2</sub> (Fig. 26(a)). HCP@SiO<sub>2</sub> NPs with amine groups, denoted HCP@SiO<sub>2</sub>-NH<sub>2</sub>, were achieved through the surface modification. The hybrid NPs were used to stain cytoplasmic regions of the living cells. The fluorescence images (Fig. 26(b)) indicated that NPs with amino groups facilitate their cellular uptake into HeLa cells. Such silica-covered FNSs offered more opportunities for further surface modification [321], which was also a strategy for site-specific targeting in bioimaging.

#### 4.3. Heavy-metal complex

Among the above-mentioned fluorescent materials, neither down conversion nor up conversion materials could emit fluorescence without excitation light. Since phosphorescence is a fluorescence phenomenon with

characteristic decay rate which could be observed after removal of the excitation light, FNSs with phosphorescence emission can be designed based on heavy-metal complexes with a unique d<sup>6</sup>, d<sup>8</sup>, and d<sup>10</sup>-electron configuration. Unlike above-mentioned organic or inorganic fluorophores, which are singlet state emitters, heavy-metal complexes are triplet emitters [322]. Since the strong metal-induced spin-orbit coupling leads to efficient singlet–triplet state mixing, the spin-forbidden nature of the irradiative relaxation of the triplet state can be avoided, resulting in highly intense phosphorescent emission at room temperature [323]. To date, heavy-metal complexes, including Re(I)-, Ru(II)-, Os(II)-, Ir(III)- and Rh(III)-complexes with d<sup>6</sup> electronic structures, Pt(II)-complexes with d<sup>8</sup> electronic structures, and Au(I)- and Cu(I)-complexes with d<sup>10</sup> electronic structures have been reported as the most important materials with phosphorescent emission at room temperature [324].

Recent studies on heavy-metal complexes with different counter ions, solvent ligands and cyclometallated ligands demonstrated the design concept with practical applications in cell imaging [325]. For instance, Tan et al. [326] reported the synthesis of an iridium(III) complex [(Py-BTE)<sub>2</sub>Ir(acac)] (Fig. 27) with switchable phosphorescence [(Py-BTE)<sub>2</sub>Ir(pic)]. The switchable phosphorescence of

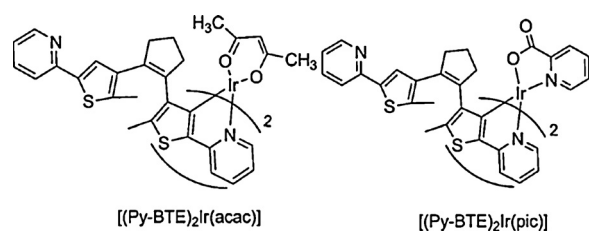


**Fig. 27.** Structures of [(Py-BTE)<sub>2</sub>Ir(acac)] and [(Py-BTE)<sub>2</sub>Ir(pic)] [326]. Copyright 2011. Adapted with permission from WILEY-VCH Verlag GmbH & Co. KGaA, Weinheim.

$[(\text{Py-BTE})_2\text{Ir(pic)}]$  in solution and within living cells could be controlled by two distinguishable visible-light irradiations. As a result, this complex showed great advantages as a phosphorescence probe for monitoring living cells.

However, toxicity limited the widespread applications of heavy metal ions. In order to solve this problem, further functionalization of heavy-metal complexes has been reported recently. When conjugated with target biomolecules, such FNSs emit strong fluorescence at longer wavelength, thus the specific labeling and recognition could be realized. For instance, Shi et al. [327] synthesized phosphorescent conjugated polyelectrolytes (PCPEs) containing Ir(III) complexes and polyfluorene units, which emitted blue fluorescence in aqueous solutions. Since electrostatic interaction between the nanoparticles and heparin could improve the energy transfer between the polyfluorene units to Ir(III) complex, the red signal could also be observed with naked-eyes (Fig. 28). Therefore, the PCPEs could be used in specific labeling of live KB cell membrane with high contrast, which could be used in both confocal fluorescent cellular imaging and fluorescence lifetime imaging microscopy.

## 5. Perspective

Due to their attractive properties, including ultra-small size, high brightness, monodispersity and low

**Table 5**

Most reported bio-distribution of FNSs for *in vivo* bioimaging.

Bio-distribution	Refs.	Bio-distribution	Refs.
Liver	[279,333,334]	Lymph nodes	[335,336]
Lung	[38,337–339]	Tumor	[340–342]
Kidney	[343–345]	Brain	[55,346–348]
Spleen	[349–351]	Skin	[352]

photobleaching, FNSs represent a highly attractive platform for bioimaging [328]. Despite their great potential and promising future as novel fluorescent probes in bioimaging, further improvement of FNSs still faces many challenges.

First, progress in the design and development of better synthesis routes for different FNSs with good target specificity are needed. The required selectivity, e.g., specific labeling cell membrane, nucleus or ECM, could be realized by surface modification through multi-functionalization [35]. And the resulted structures should have special chemical or physical conjugation between FNSs and the targeted biotic components [329], e.g., macromolecules, subcellular organelles, specific cancer cells and so on. In the real *in vivo* bioimaging application, the bio-distribution of FNSs is an important point, which is dependent upon the composition or surface modification of FNSs, and the physiological environments [267,330–332] (Table 5). Up to present, liver and kidney were found to have excellent affinity with most FNSs although their real targeted bio-distribution is still a

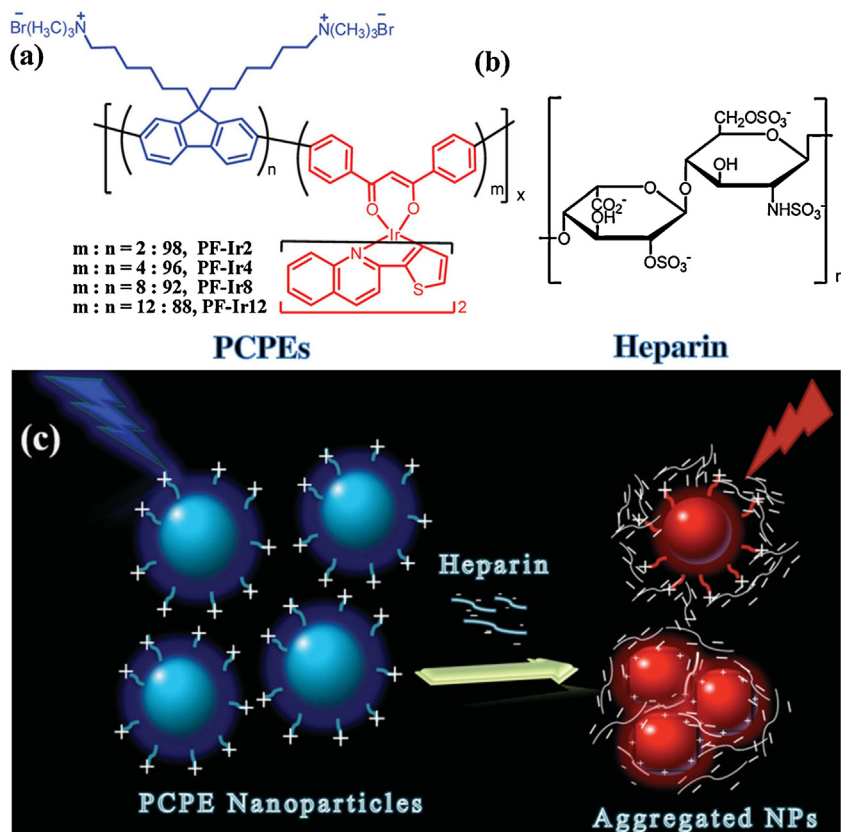


**Fig. 28.** Structures of the synthetic (a) PCPEs and (b) heparin; (c) the possible sensing mechanism [327]. Copyright 2013. Adapted with permission from WILEY-VCH Verlag GmbH & Co. KGaA, Weinheim.

great challenge. Further effort could be made in improving the functionality of complex for better stability and sensitivity in both cellular and tissue levels.

Second, FNSs should be simultaneously functionalized with other properties in addition to fluorescence. With the development and maturity of fluorescent probes in the last decades, there is a great demand on their general-purpose optimal design [353]. In addition to the application in biolabeling, FNSs in other fields, such as biological recognition, separation, orientation, delivery, bio-thermal and chemical sensors [239,354,355], are also explored. And diversification of fluorescent nanostructure design for multiple bioactivities has always been the trend of bio-science and technology development.

Third, to be fully accepted in the field of nanobiotechnology, careful investigation on the safety of FNSs in bioimaging is still needed [356]. Since bioimaging is mostly performed *in vivo*, there is an increasing concern about the toxic effects of synthetic FNSs in humans. The toxicity of FNSs is dependent on the following two factors [357,358]: (1) chemical composition of FNSs. For instance, quantum dots contain toxic cadmium (CdSe, CdS, etc.). However, potential toxicity could be avoided by coating to control the release of toxic elements [359,360]. (2) Morphology or structure of FNSs. Toxicological data from animal tests suggest that some FNSs could exert adverse effects in animals due to the retention of FNSs inside animal bodies. Therefore, it would be preferable that the sizes of FNSs are smaller than the threshold of renal metabolism [361]. In order to remove these nanostructures from cells and animals efficiently, ultrafine functionalized FNSs should be prepared in the future.

Fourth, developing fluorescent probes working for first or second biological windows (up to 1400 nm) seems to be quite important. To date, fluorescence imaging of deep tissue has been significantly hindered because of the insufficient tissue light transmission and high scattering. NIR light (700–2500 nm) can penetrate biological tissues, such as skin and blood, more efficiently than visible light [362]. Therefore, it is a challenge to prepare FNSs that could perform bioimaging in the long wavelength region (NIR region). Fluorescent nanoprobes for deep tissue *in vivo* imaging should possess following properties: (1) non-toxicity; (2) both the excitation light and fluorescent emission in the spectral range which is favorable for the penetration of light through thick tissues; (3) efficient and stable fluorescence signal. Up to present, FNSs for deep tissue imaging is gaining increasing attention, and preponderant candidates, such as carbon nanotubes, two-photon metallic NCs, and UCNPs, have been investigated for bioimaging application.

## 6. Summary

We summarize the extensive efforts on the development of FNSs, which have attractive features for their applications in bioimaging. In this review, we first introduce three classifications of bioimaging FNSs according to their chemical compositions. Their specific structural designs, synthetic strategies and the size effects on the optical properties are subsequently summarized. Great efforts

have been made to improve their fluorescence intensity, specificity in targeting, biocompatibility and non-toxicity, etc. Although many FNSs have been synthesized and applied biologically, there are still much to be done before they could be widely used as fluorescent probes in clinical tests. With further advances in the design and synthesis of multifunctional FNSs with high quality, the widespread application of FNSs could be expected not only in advanced bioimaging, but also in ultrasensitive molecular diagnosis, novel light-emitting nanodevices and intracellular drug delivery.

## Acknowledgements

The authors acknowledge the financial support of the “National Science Foundation of China” (21174012, 51103008, 51221002) and the “New Century Excellent Talents Award Program, Ministry of Education, China (NCET-10-0215)” and the Doctoral Program of Higher Education Research Fund (20100010120006, 20120010110008).

## References

- [1] Kikuchi K. Design, synthesis and biological application of chemical probes for bioimaging. *Chem Soc Rev* 2010;39:2048–53.
- [2] Azhdarinia A, Ghosh P, Ghosh S, Wilgowski N, Sevick-Muraca EM. Dual-labeling strategies for nuclear and fluorescence molecular imaging: a review and analysis. *Mol Imaging Biol* 2012;14:261–76.
- [3] De M, Ghosh PS, Rotello VM. Applications of nanoparticles in biology. *Adv Mater* 2008;20:4225–41.
- [4] Hahn MA, Singh AK, Sharma P, Brown SC, Moudgil BM. Nanoparticles as contrast agents for *in-vivo* bioimaging: current status and future perspectives. *Anal Bioanal Chem* 2011;399:3–27.
- [5] Liu J, Yang X, He X, Wang K, Wang Q, Guo Q, Shi H, Huang J, Huo X. Fluorescent nanoparticles for chemical and biological sensing. *Sci China Chem* 2011;54:1157–76.
- [6] Jańczewski D, Zhang Y, Das GK, Yi DK, Padmanabhan P, Bhakoo KK, Tan TTY, Selvan ST. Bimodal magnetic-fluorescent probes for bioimaging. *Microsc Res Tech* 2011;74:563–76.
- [7] Wang L, Zhu X, Xie C, Ding N, Weng X, Lu W, Wei X, Li C. Imaging acidosis in tumors using a pH-activated near-infrared fluorescence probe. *Chem Commun* 2012;48:11677–9.
- [8] Li K, Liu B. Polymer encapsulated conjugated polymer nanoparticles for fluorescence bioimaging. *J Mater Chem* 2012;22:1257–64.
- [9] Zeng S, Tsang MK, Chan CF, Wong KL, Hao J. PEG modified BaGdF5: Yb/Er nanoprobes for multi-modal upconversion fluorescent, *in vivo* X-ray computed tomography and biomagnetic imaging. *Biomaterials* 2012;33:9232–8.
- [10] Yang T, Liu Q, Pu S, Dong Z, Huang C, Li F. Fluorophore-photochrome co-embedded polymer nanoparticles for photoswitchable fluorescence bioimaging. *Nano Res* 2012;5:494–503.
- [11] Kim JH, Park K, Nam HY, Lee S, Kim K, Kwon IC. Polymers for bioimaging. *Prog Polym Sci* 2007;32:1031–53.
- [12] Tian H, Tang Z, Zhuang X, Chen X, Jing X. Biodegradable synthetic polymers: preparation, functionalization and biomedical application. *Prog Polym Sci* 2012;37:237–80.
- [13] Cha C, Shin SR, Annabi N, Dokmeci MR, Khademhosseini A. Carbon-based nanomaterials: multifunctional materials for biomedical engineering. *ACS Nano* 2013;7:2891–7.
- [14] Magrez A, Kasas S, Salicio V, Pasquier N, Seo JW, Celio M, Catsicas S, Schwaller B, Forró L. Cellular toxicity of carbon-based nanomaterials. *Nano Lett* 2006;6:1121–5.
- [15] Ray S, Saha A, Jana NR, Sarkar R. Fluorescent carbon nanoparticles: synthesis, characterization, and bioimaging application. *J Phys Chem C* 2009;113:18546–51.
- [16] Sahu S, Behera B, Maiti TK, Mohapatra S. Simple one-step synthesis of highly luminescent carbon dots from orange juice: application as excellent bioimaging agents. *Chem Commun* 2012;48:8835–7.
- [17] Shen L, Zhang L, Chen M, Chen X, Wang J. The production of pH-sensitive photoluminescent carbon nanoparticles by the carbonization of polyethylenimine and their use for bioimaging. *Carbon* 2013;5:343–9.

- [18] Zhu S, Meng Q, Wang L, Zhang J, Song Y, Jin H, Zhang K, Sun H, Wang H, Yang B. Highly photoluminescent carbon dots for multicolor patterning, sensors, and bioimaging. *Angew Chem* 2013;125:4045–9.
- [19] Shen J, Zhu Y, Yang X, Li C. Graphene quantum dots: emergent nanolights for bioimaging, sensors, catalysis and photovoltaic devices. *Chem Commun* 2012;48:3686–99.
- [20] Zhu S, Zhang J, Qiao C, Tang S, Li Y, Yuan W, Li B, Tian L, Liu F, Hu R. Strongly green-photoluminescent graphene quantum dots for bioimaging applications. *Chem Commun* 2011;47:6858–60.
- [21] Cao L, Wang X, Meziani MJ, Lu F, Wang H, Luo PG, Lin Y, Harruff BA, Veca LM, Murray D. Carbon dots for multiphoton bioimaging. *J Am Chem Soc* 2007;129:11318–9.
- [22] Yang ST, Wang X, Wang H, Lu F, Luo PG, Cao L, Meziani MJ, Liu JH, Liu Y, Chen M. Carbon dots as nontoxic and high-performance fluorescence imaging agents. *J Phys Chem C* 2009;113:18110–4.
- [23] Qian Z, Ma J, Shan X, Shao L, Zhou J, Chen J, Feng H. Surface functionalization of graphene quantum dots with small organic molecules from photoluminescence modulation to bioimaging applications: an experimental and theoretical investigation. *RSC Adv* 2013;3:14571–9.
- [24] Luo PG, Sahu S, Yang ST, Sonkar SK, Wang J, Wang H, LeCroy GE, Cao L, Sun YP. Carbon “quantum” dots for optical bioimaging. *J Mater Chem* B 2013;1:2116–27.
- [25] Bhunia SK, Saha A, Maity AR, Ray SC, Jana NR. Carbon nanoparticle-based fluorescent bioimaging probes. *Sci Rep* 2013;3, 1473/1–7.
- [26] Ding C, Zhu A, Tian Y. Functional surface engineering of C-dots for fluorescent biosensing and in vivo bioimaging. *Acc Chem Res* 2013, <http://dx.doi.org/10.1021/ar400023s>.
- [27] Moon HK, Lee SH, Choi HC. In vivo near-infrared mediated tumor destruction by photothermal effect of carbon nanotubes. *ACS Nano* 2009;3:3707–13.
- [28] Lacerda L, Raffa S, Prato M, Bianco A, Kostarelos K. Cell-penetrating CNTs for delivery of therapeutics. *Nano Today* 2007;2:38–43.
- [29] Barone PW, Baik S, Heller DA, Strano MS. Near-infrared optical sensors based on single-walled carbon nanotubes. *Nat Mater* 2004;4:86–92.
- [30] Harrison BS, Atala A. Carbon nanotube applications for tissue engineering. *Biomaterials* 2007;28:344–53.
- [31] Zhang Y, Valley N, Brozena AH, Piao Y, Song X, Schatz GC, Wang Y. Propagative sidewall alkylcarboxylation that induces red-shifted near-IR photoluminescence in single-walled carbon nanotubes. *J Phys Chem Lett* 2013;4:826–30.
- [32] Cherukuri P, Bachilo SM, Litovsky SH, Weisman RB. Near-infrared fluorescence microscopy of single-walled carbon nanotubes in phagocytic cells. *J Am Chem Soc* 2004;126:15638–9.
- [33] Robinson JT, Welsher K, Tabakman SM, Sherlock SP, Wang H, Luong R, Dai H. High performance in vivo near-IR (>1 μm) imaging and photothermal cancer therapy with carbon nanotubes. *Nano Res* 2010;3:779–93.
- [34] O’Connell MJ, Bachilo SM, Huffman CB, Moore VC, Strano MS, Haroz EH, Rialon KL, Boul PJ, Noon WH, Kittrell C. Band gap fluorescence from individual single-walled carbon nanotubes. *Science* 2002;297:593–6.
- [35] Chan J, Dodani SC, Chang CJ. Reaction-based small-molecule fluorescent probes for chemoselective bioimaging. *Nat Chem* 2012;4:973–84.
- [36] Yuan L, Lin W, Zheng K, Zhu S. FRET-based small-molecule fluorescent probes: rational design and bioimaging applications. *Acc Chem Res* 2013;46:1462–73.
- [37] Tera T, Nagano T. Small-molecule fluorophores and fluorescent probes for bioimaging. *Pflug Arch Eur J Phys* 2013;465:347–59.
- [38] Chen X, Nam SW, Kim GH, Song N, Jeong Y, Shin I, Kim SK, Kim J, Park S, Yoon J. A near-infrared fluorescent sensor for detection of cyanide in aqueous solution and its application for bioimaging. *Chem Commun* 2010;46:8953–5.
- [39] Guo Z, Nam S, Park S, Yoon J. A highly selective ratiometric near-infrared fluorescent cyanine sensor for cysteine with remarkable shift and its application in bioimaging. *Chem Sci* 2012;3:2760–5.
- [40] Li X, Qian S, He Q, Yang B, Li J, Hu Y. Design and synthesis of a highly selective fluorescent turn-on probe for thiol bioimaging in living cells. *Org Biomol Chem* 2010;8:3627–30.
- [41] Adronov A, Frechet JM, He GS, Kim KS, Chung SJ, Swiatkiewicz J, Prasad PN. Novel two-photon absorbing dendritic structures. *Chem Mater* 2000;12:2838–41.
- [42] Ftouni H, Bolze Fdr, de Rocquigny H, Nicoud JF. Functionalized two-photon absorbing diketopyrrolopyrrole-based fluorophores for living cells fluorescent microscopy. *Bioconjugate Chem* 2013;24:942–50.
- [43] Wong MS, Yang W, Chan PS, Chan MS, Li KF, Lo PK, Mak NK, Kok wai C. Two-photon fluorescence probes for imaging of mitochondria and lysosomes. *Chem Commun* 2013;49:3428–30.
- [44] Monnereau C, Marotte S, Lanôe PH, Maury O, Baldeck PL, Kreher D, Favier A, Charreyre MT, Marvel J, Leverrier Y. Water-soluble chromophores with star-shaped oligomeric arms: synthesis, spectroscopic studies and first results in bioimaging and cell death induction. *New J Chem* 2012;36:2328–33.
- [45] Song HO, Lee B, Bhusal RP, Park B, Yu K, Chong CK, Cho P, Kim SY, Kim HS, Park H. Development of a novel fluorophore for real-time biomonitoring system. *PLoS ONE* 2012;7, e48459/1–10.
- [46] Cao X, Lin W, Yu Q. A ratiometric fluorescent probe for thiols based on a tetrakis(4-hydroxyphenyl) porphyrin-coumarin scaffold. *J Org Chem* 2011;76:7423–30.
- [47] Serin JM, Brousse DW, Fréchet JM. A FRET-based ultraviolet to near-infrared frequency converter. *J Am Chem Soc* 2002;124:11848–9.
- [48] Albertazzi L, Storti B, Marchetti L, Beltram F. Delivery and subcellular targeting of dendrimer-based fluorescent pH sensors in living cells. *J Am Chem Soc* 2010;132:18158–67.
- [49] Han L, Li J, Huang S, Huang R, Liu S, Hu X, Yi P, Shan D, Wang X, Lei H. Peptide-conjugated polyamidoamine dendrimer as a nanoscale tumor-targeted T1 magnetic resonance imaging contrast agent. *Biomaterials* 2011;32:2989–98.
- [50] Hayek A, Bolze Fdr, Bourgogne C, Baldeck PL, Didier P, Arntz Y, Mély Y, Nicoud JF. Boron containing two-photon absorbing chromophores. 2. Fine tuning of the one- and two-photon photophysical properties of pyrazabole based fluorescent bioprobes. *Inorg Chem* 2009;48:9112–9.
- [51] Tsai HC, Imae T, Calderó G, Solans C. Two-photon confocal imaging study: cell uptake of two photon dyes-labeled PAMAM dendrons in HeLa cells. *J Biomed Mater Res A* 2012;100:746–56.
- [52] Srikan D, Albers AE, Chang CJ. A dendrimer-based platform for simultaneous dual fluorescence imaging of hydrogen peroxide and pH gradients produced in living cells. *Chem Sci* 2011;2:1156–65.
- [53] Chen J, Tian H, Guo Z, Lin L, Dong X, Zhu X, Chen X. Hyperbranched PEI grafted by hydrophilic amino acid segment poly[N-(2-hydroxyethyl)-L-glutamine] as an efficient nonviral gene carrier. *J Appl Polym Sci* 2012;123:2257–65.
- [54] Ding D, Wang G, Liu J, Li K, Pu KY, Hu Y, Ng JC, Tang BZ, Liu B. Hyperbranched conjugated polyelectrolyte for dual-modality fluorescence and magnetic resonance cancer imaging. *Small* 2012;8:3523–30.
- [55] Janaszewska A, Ziembka B, Ciepluch K, Appelhans D, Voit B, Klajnert B, Bryszewska M. The biodistribution of maltotriose modified poly(propylene imine) (PPI) dendrimers conjugated with fluorescein-proofs of crossing blood-brain-barrier. *New J Chem* 2012;36:350–3.
- [56] Pereira VH, Salgado A, Oliveira JM, Cerqueira SR, Frias A, Fraga J, Roque S, Falcão AM, Marques F, Neves N. In vivo biodistribution of carboxymethylchitosan/poly(amidoamine) dendrimer nanoparticles in rats. *J Bioact Compat Polym* 2011;26:619–27.
- [57] Yan H, Wang J, Yi P, Lei H, Zhan C, Xie C, Feng L, Qian J, Zhu J, Lu W. Imaging brain tumor by dendrimer-based optical/paramagnetic nanoprobe across the blood-brain barrier. *Chem Commun* 2011;47:8130–2.
- [58] Samuelson LE, Dukes MJ, Hunt CR, Casey JD, Bornhop DJ. TSPO targeted dendrimer imaging agent: synthesis, characterization, and cellular internalization. *Bioconjugate Chem* 2009;20:2082–9.
- [59] Pang Y, Zhu Q, Liu J, Wu J, Wang R, Chen S, Zhu X, Yan D, Huang W, Zhu B. Design and synthesis of cationic drug carriers based on hyperbranched poly(amine-ester)s. *Biomacromolecules* 2010;11:575–82.
- [60] Xu Z, He B, Shen J, Yang W, Yin M. Fluorescent water-soluble perylenediimide-cored cationic dendrimers: synthesis, optical properties, and cell uptake. *Chem Commun* 2013;49:3646–8.
- [61] Heek T, Fasting C, Rest C, Zhang X, Würthner F, Haag R. Highly fluorescent water-soluble polyglycerol-dendronized perylene bisimide dyes. *Chem Commun* 2010;46:1884–6.
- [62] Yang SK, Shi X, Park S, Doganay S, Ha T, Zimmerman SC. Monovalent, clickable, uncharged, water-soluble perylenediimide-cored dendrimers for target-specific fluorescent biolabeling. *J Am Chem Soc* 2011;133:9964–7.
- [63] Yang SK, Zimmerman SC. Polyglycerol-dendronized perylenediimides as stable, water-soluble fluorophores. *Adv Funct Mater* 2012;22:3023–8.
- [64] Gao B, Li H, Liu H, Zhang L, Bai Q, Ba X. Water-soluble and fluorescent dendritic perylene bisimides for live-cell imaging. *Chem Commun* 2011;47:3894–6.

- [65] Zill AT, Licha K, Haag R, Zimmerman SC. Synthesis and properties of fluorescent dyes conjugated to hyperbranched polyglycerols. *New J Chem* 2012;36:419–27.
- [66] Olson ES, Jiang T, Aguilera TA, Nguyen QT, Ellies LG, Scadeng M, Tsien RY. Activatable cell penetrating peptides linked to nanoparticles as dual probes for *in vivo* fluorescence and MR imaging of proteases. *PNAS* 2010;107:4311–6.
- [67] Kim Y, Kim SH, Tanyeri M, Katzenellenbogen JA, Schroeder CM. Dendrimer probes for enhanced photostability and localization in fluorescence imaging. *Biophys J* 2013;104:1566–75.
- [68] Iezzi R, Guru BR, Glybina IV, Mishra MK, Kennedy A, Kannan RM. Dendrimer-based targeted intravitreal therapy for sustained attenuation of neuroinflammation in retinal degeneration. *Biomaterials* 2012;33:979–88.
- [69] Tanaka K, Siwu ER, Minami K, Hasegawa K, Nozaki S, Kanayama Y, Koyama K, Chen WC, Paulson JC, Watanabe Y. Noninvasive imaging of dendrimer-type N-glycan clusters: *in vivo* dynamics dependence on oligosaccharide structure. *Angew Chem Int Ed* 2010;49:1895–200.
- [70] Li J, Guo K, Shen J, Yang W, Yin M. A difunctional squarylium indocyanine dye distinguishes dead cells through diverse staining of the cell nuclei/membranes. *Small* 2013; <http://dx.doi.org/10.1002/smll.201302920>.
- [71] Li J, Ji C, Yang W, Yin M. pH switchable and fluorescent ratiometric squarylium indocyanine dyes as extremely alkaline solution sensors. *Analyst* 2013;138:7289–93.
- [72] Andrade CD, Yanez CO, Rodriguez L, Belfield KD. A series of fluorene-based two-photon absorbing molecules: synthesis, linear and nonlinear characterization, and bioimaging. *J Org Chem* 2010;75:3975–82.
- [73] Chen CY, Tian Y, Cheng YJ, Young AC, Ka JW, Jen AKY. Two-photon absorbing block copolymer as a nanocarrier for porphyrin: energy transfer and singlet oxygen generation in micellar aqueous solution. *J Am Chem Soc* 2007;129:7220–1.
- [74] Trohalaki S, Kedziora GS, Pachter R. Molecular dynamics simulation of two photon-absorbing polyimides: evidence for the formation of intra- and inter-chain dimers. *Polymer* 2012;53:3421–5.
- [75] Yang Z, Zhao N, Sun Y, Miao F, Liu Y, Liu X, Zhang Y, Ai W, Song G, Shen X. Highly selective red-and green-emitting two-photon fluorescent probes for cysteine detection and their bioimaging in living cells. *Chem Commun* 2012;48:3442–4.
- [76] Zhu Q, Qiu F, Zhu B, Zhu X. Hyperbranched polymers for bioimaging. *RSC Adv* 2013;3:2071–83.
- [77] Wijagkanalan W, Kawakami S, Hashida M. Designing dendrimers for drug delivery and imaging: pharmacokinetic considerations. *Pharm Res* 2011;28:1500–19.
- [78] Merkel OM, Zheng M, Mintzer MA, Pavan GM, Librizzi D, Maly M, Höffken H, Danani A, Simanek EE, Kissel T. Molecular modeling and *in vivo* imaging can identify successful flexible triazine dendrimer-based siRNA delivery systems. *J Control Release* 2011;153:23–33.
- [79] Wang G, Yin H, Ng JC, Cai L, Li J, Tang BZ, Liu B. Polyethyleneimine-grafted hyperbranched conjugated polyelectrolytes: synthesis and imaging of gene delivery. *Polym Chem* 2013;4:5297–304.
- [80] Ping Y, Wu DC, Kumar JN, Cheng W, Lay CL, Liu Y. Redox-responsive hyperbranched poly(amine amide)s with tertiary amino cores for gene delivery. *Biomacromolecules* 2013;14:2083–94.
- [81] Feng G, Liang J, Liu B. Hyperbranched conjugated polyelectrolytes for biological sensing and imaging. *Macromol Rapid Commun* 2013;34:705–15.
- [82] Feng G, Ding D, Liu B. Fluorescence bioimaging with conjugated polyelectrolytes. *Nanoscale* 2012;4:6150–65.
- [83] Pu KY, Liu B. Fluorescent conjugated polyelectrolytes for bioimaging. *Adv Funct Mater* 2011;21:3408–23.
- [84] Pu KY, Shi J, Cai L, Li K, Liu B. Affibody-attached hyperbranched conjugated polyelectrolyte for targeted fluorescence imaging of HER2-positive cancer cell. *Biomacromolecules* 2011;12:2966–74.
- [85] Inoue Y, Kurihara R, Tsuchida A, Hasegawa M, Nagashima T, Mori T, Niidome T, Katayama Y, Okitsu O. Efficient delivery of siRNA using dendritic poly(L-lysine) for loss-of-function analysis. *J Control Release* 2008;126:59–66.
- [86] Svenson S. Dendrimers as versatile platform in drug delivery applications. *Eur J Pharm Biopharm* 2009;71:445–62.
- [87] Yang SK, Shi X, Park S, Ha T, Zimmerman SC. A dendritic single-molecule fluorescent probe that is monovalent, photostable and minimally blinking. *Nat Chem* 2013;5:692–7.
- [88] Bao Y, Wang H, Li Q, Liu B, Bai W, Jin B, Bai R. 2,2'-Biimidazole-based conjugated polymers as a novel fluorescent sensing platform for pyrophosphate anion. *Macromolecules* 2012;45:3394–401.
- [89] Gu PY, Lu CJ, Xu QF, Ye GJ, Chen WQ, Duan XM, Wang LH, Lu JM. Star-shaped polymer PFStODO by atom transfer radical polymerization: its synthesis, characterization, and fluorescence property. *J Polym Sci, A: Polym Chem* 2012;50:480–7.
- [90] Hoffmann S, Vystrčilová L, Ulbrich K, Etrych T, Caysa H, Mueller T, Mäder K. Dual fluorescent HPMA copolymers for passive tumour targeting with pH-sensitive drug release: synthesis and characterisation of distribution and tumour accumulation in mice by noninvasive multispectral optical imaging. *Biomacromolecules* 2012;13:652–63.
- [91] Benoit D, Chaplinski V, Braslav R, Hawker CJ. Development of a universal alkoxyamine for “living” free radical polymerizations. *J Am Chem Soc* 1999;121:3904–20.
- [92] Darling TR, Davis TP, Fryd M, Gridnev AA, Haddleton DM, Ittel SD, Matheson RR, Moad G, Rizzardo E. Living polymerization: rationale for uniform terminology. *J Polym Sci, A: Polym Chem* 2000;38:1706–8.
- [93] Krstina J, Moad G, Rizzardo E, Winzor CL, Berge CT, Fryd M. Narrow polydispersity block copolymers by free-radical polymerization in the presence of macromonomers. *Macromolecules* 1995;28:5381–5.
- [94] Moad G, Chen M, Häussler M, Postma A, Rizzardo E, Thang SH. Functional polymers for optoelectronic applications by RAFT polymerization. *Polym Chem* 2011;2:492–519.
- [95] Moad G, Rizzardo E, Thang SH. RAFT polymerization and some of its applications. *Chem Asian J* 2013;8:1634–44.
- [96] Moad G, Rizzardo E, Thang SH. Toward living radical polymerization. *Acc Chem Res* 2008;41:1133–42.
- [97] Siegwart DJ, Oh JK, Matyjaszewski K. ATRP in the design of functional materials for biomedical applications. *Prog Polym Sci* 2012;37:18–37.
- [98] Gao H, Matyjaszewski K. Synthesis of functional polymers with controlled architecture by CRP of monomers in the presence of cross-linkers: from stars to gels. *Prog Polym Sci* 2009;34:317–50.
- [99] Braunecker WA, Matyjaszewski K. Controlled/living radical polymerization: features, developments, and perspectives. *Prog Polym Sci* 2007;32:93–146.
- [100] Yin M, Kuhlmann CR, Sorokina K, Li C, Mihov G, Pietrowski E, Koynov K, Klapper M, Luhmann HJ, Müllen K, Weil T. Novel fluorescent core-shell nanocantainers for cell membrane transport. *Biomacromolecules* 2008;9:1381–9.
- [101] Yin M, Ding K, Gropeanu RA, Shen J, Berger R, Weil T, Müllen K. Dendritic star polymers for efficient DNA binding and stimulus-dependent DNA release. *Biomacromolecules* 2008;9:3231–8.
- [102] Yin M, Shen J, Pflugfelder GO, Müllen K. A fluorescent core-shell dendritic macromolecule specifically stains the extracellular matrix. *J Am Chem Soc* 2008;130:7806–7.
- [103] Yin M, Shen J, Pisula W, Liang M, Zhi L, Müllen K. Functionalization of self-assembled hexa-peri-hexabenzocoronene fibers with peptides for bioprobing. *J Am Chem Soc* 2009;131:14618–9.
- [104] Yin M, Cheng Y, Liu M, Gutmann JS, Müllen K. Nanostructured TiO<sub>2</sub> films templated by amphiphilic dendritic core-double-shell macromolecules: from isolated nanorings to continuous 2D mesoporous networks. *Angew Chem Int Ed* 2008;47:8400–3.
- [105] Yin M, Shen J, Gropeanu R, Pflugfelder GO, Weil T, Müllen K. Fluorescent core/shell nanoparticles for specific cell-nucleus staining. *Small* 2008;4:894–8.
- [106] Chen S, Duhamel J, Bahun GJ, Adronov A. Quantifying the presence of unwanted fluorescent species in the study of pyrene-labeled macromolecules. *J Phys Chem B* 2011;115:9921–9.
- [107] Barrett T, Ravizzini G, Choyke P, Kobayashi H. Dendrimers in medical nanotechnology. *IEEE Eng Med Biol* 2009;28:12–22.
- [108] Li J, Yang J, Xu F, Xu J, Yan D, Chen C, Li J. A facile strategy to modulate the fluorescent properties of star polymers by varying the arm numbers. *J Polym Res* 2012;19:9941–4.
- [109] Chu CC, Imae T. Fluorescence investigations of oxygen-doped simple amine compared with fluorescent PAMAM dendrimer. *Macromol Rapid Commun* 2009;30:89–93.
- [110] Jayamurugan G, Umesh C, Jayaraman N. Inherent photoluminescence properties of poly(propyl ether imine) dendrimers. *Org Lett* 2008;10:9–12.
- [111] Sun M, Hong C, Pan C. A unique aliphatic tertiary amine chromophore: fluorescence, polymer structure, and application in cell imaging. *J Am Chem Soc* 2012;134:20581–4.
- [112] Shen Y, Ma X, Zhang B, Zhou Z, Sun Q, Jin E, Sui M, Tang J, Wang J, Fan M. Degradable dual pH- and temperature-responsive photoluminescent dendrimers. *Chem Eur J* 2011;17:5319–26.
- [113] Wu D, Liu Y, He C, Goh SH. Blue photoluminescence from hyperbranched poly(amine ester)s. *Macromolecules* 2005;38:9906–9.

- [114] Tsai YJ, Hu CC, Chu CC, Imae T. Intrinsically fluorescent PAMAM dendrimer as gene carrier and nanoprobe for nucleic acids delivery: bioimaging and transfection study. *Biomacromolecules* 2011;12:4283–90.
- [115] Yang W, Pan C, Liu X, Wang J. Multiple functional hyperbranched poly(amido amine) nanoparticles: synthesis and application in cell imaging. *Biomacromolecules* 2011;12:1523–31.
- [116] Wang Y, Hong C, Pan C. Spiropyran-based hyperbranched star copolymer: synthesis, phototropy, FRET, and bioapplication. *Biomacromolecules* 2012;13:2585–93.
- [117] Yang W, Pan C, Luo M, Zhang H. Fluorescent mannose-functionalized hyperbranched poly(amido amine)s: synthesis and interaction with *E. coli*. *Biomacromolecules* 2010;11:1840–6.
- [118] Beecroft RA, Davidson RS, Whelan TD. Fluorescent excimer formation by  $\alpha,\omega$ -diaminoalkanes and related compounds. *J Chem Soc, Perkin Trans 1985*;2:1069–72.
- [119] Freeman C, McEwan M, Claridge R, Phillips L. Fluorescence of aliphatic amines. *Chem Phys Lett* 1971;8:77–8.
- [120] Chen J, Zhang P, Fang G, Yi P, Zeng F, Wu S. Design and synthesis of FRET-mediated multicolor and photoswitchable fluorescent polymer nanoparticles with tunable emission properties. *J Phys Chem B* 2012;116:4354–62.
- [121] Zhu L, Wu W, Zhu M, Han JJ, Hurst JK, Li AD. Reversibly photoswitchable dual-color fluorescent nanoparticles as new tools for live-cell imaging. *J Am Chem Soc* 2007;129:3524–6.
- [122] Zandanel C, Vauthier C. Characterization of fluorescent poly(isobutylcyanoacrylate) nanoparticles obtained by copolymerization of a fluorescent probe during redox radical emulsion polymerization (RREP). *Eur J Pharm Biopharm* 2012;82:66–75.
- [123] Goto C, Okabe K, Funatsu T, Harada Y, Uchiyama S. Hydrophilic fluorescent nanogel thermometer for intracellular thermometry. *J Am Chem Soc* 2009;131:2766–7.
- [124] Chen J, Zhang P, Fang G, Yi P, Yu X, Li X, Zeng F, Wu S. Synthesis and characterization of novel reversible photoswitchable fluorescent polymeric nanoparticles via one-step miniemulsion polymerization. *J Phys Chem B* 2011;115:3354–62.
- [125] Chen Y, Wilbon PA, Zhou J, Nagarkatti M, Wang C, Chu F, Tang C. Multifunctional self-fluorescent polymer nanogels for label-free imaging and drug delivery. *Chem Commun* 2013;49:297–9.
- [126] Relogio P, Bathfield M, Haftek Terreau Z, Beija M, Favier A, Giraud Panis MJ, D'Agosto F, Mandrand B, Farinha JPS, Charreyre MT. Biotin-end-functionalized highly fluorescent water-soluble polymers. *Polym Chem* 2013;4:2909–3148.
- [127] Martin V, Banuelos J, Enciso E, LopezArbeloa I, Costela Á, Garcia-Moreno I. Photophysical and lasing properties of rhodamine 6G confined in polymeric nanoparticles. *J Phys Chem C* 2011;115:3926–33.
- [128] Oh WK, Jeong YS, Kim S, Jang J. Fluorescent polymer nanoparticle for selective sensing of intracellular hydrogen peroxide. *ACS Nano* 2012;6:8516–24.
- [129] Fernando LP, Kandel PK, Yu J, McNeill J, Ackroyd PC, Christensen KA. Mechanism of cellular uptake of highly fluorescent conjugated polymer nanoparticles. *Biomacromolecules* 2010;11:2675–82.
- [130] Patra A, Koenen JM, Scherf U. Fluorescent nanoparticles based on a microporous organic polymer network: fabrication and efficient energy transfer to surface-bound dyes. *Chem Commun* 2011;47:9612–4.
- [131] Dossi M, Ferrari R, Dragoni L, Martignoni C, Gaetani P, D'Incalci M, Morbidelli M, Moscatelli D. Synthesis of fluorescent PMMA-based nanoparticles. *Macromol Mater Eng* 2012;298:771–8.
- [132] Sauer R, Turshatov A, Balushev S, Landfester K. One-pot production of fluorescent surface-labeled polymeric nanoparticles via miniemulsion polymerization with BODIPY surfmers. *Macromolecules* 2012;45:3787–96.
- [133] Yoo L, Park JS, Kwon KC, Kim SE, Jin X, Kim H, Lee J. Fluorescent viral nanoparticles with stable in vitro and in vivo activity. *Biomaterials* 2012;33:6194–200.
- [134] Buck SM, Xu H, Brasuel M, Philbert MA, Kopelman R. Nanoscale probes encapsulated by biologically localized embedding (PEBBLES) for ion sensing and imaging in live cells. *Talanta* 2004;63:41–59.
- [135] Siegwart DJ, Srinivasan A, Bencherif SA, Karunandhi A, Oh JK, Vaidya S, Jin R, Hollinger JO, Matyjaszewski K. Cellular uptake of functional nanogels prepared by inverse miniemulsion ATRP with encapsulated proteins, carbohydrates, and gold nanoparticles. *Biomacromolecules* 2009;10:2300–9.
- [136] Kondrashina AV, Dmitriev RI, Borisov SM, Klimant I, O'Brien I, Nolan YM, Zhdanov AV, Papkovsky DB. A phosphorescent nanoparticle-based probe for sensing and imaging of (intra) cellular oxygen in multiple detection modalities. *Adv Funct Mater* 2012;22:4931–9.
- [137] Zhang L, Lin Y, Zhang Y, Chen R, Zhu Z, Wu W, Jiang X. Fluorescent micelles based on star amphiphilic copolymer with a porphyrin core for bioimaging and drug delivery. *Macromol Biosci* 2012;12:83–92.
- [138] Liu Y, Li C, Wang HY, Zhang XZ, Zhuo RX. Synthesis of thermo- and pH-sensitive polyion complex micelles for fluorescent imaging. *Chem Eur J* 2012;18:2297–304.
- [139] Lu H, Su F, Mei Q, Zhou X, Tian Y, Tian W, Johnson RH, Meldrum DR. A series of poly[N-(2-hydroxypropyl) methacrylamide] copolymers with anthracene-derived fluorophores showing aggregation-induced emission properties for bioimaging. *J Polym Sci, A: Polym Chem* 2012;50:890–9.
- [140] Wei H, Zhuo RX, Zhang XZ. Design and development of polymeric micelles with cleavable links for intracellular drug delivery. *Prog Polym Sci* 2013;38:503–35.
- [141] Niece KL, Hartgerink JD, Donners JJ, Stupp SI. Self-assembly combining two bioactive peptide-amphiphile molecules into nanofibers by electrostatic attraction. *J Am Chem Soc* 2003;125:7146–7.
- [142] Zhao Q, Li K, Chen S, Qin A, Ding D, Zhang S, Liu Y, Liu B, Sun JZ, Tang BZ. Aggregation-induced red-NIR emission organic nanoparticles as effective and photostable fluorescent probes for bioimaging. *J Mater Chem* 2012;22:15128–35.
- [143] Liu D, Feyter SD, Cotlet M, Wiesler UM, Weil T, Herrmann A, Müllen K, De Schryver FC. Fluorescent self-assembled polyphenylene dendrimer nanofibers. *Macromolecules* 2003;36:8489–98.
- [144] Luo J, Lei T, Wang L, Ma Y, Cao Y, Wang J, Pei J. Highly fluorescent rigid supramolecular polymeric nanowires constructed through multiple hydrogen bonds. *J Am Chem Soc* 2009;131:2076–7.
- [145] Yin M, Feng C, Shen J, Yu Y, Xu Z, Yang W, Knoll W, Müllen K. Dual-responsive interaction to detect DNA on template-based fluorescent nanotubes. *Small* 2011;7:1629–34.
- [146] Cui K, Lu X, Cui W, Wu J, Chen X, Lu Q. Fluorescent nanoparticles assembled from a poly(ionic liquid) for selective sensing of copper ions. *Chem Commun* 2011;47:920–2.
- [147] Hu J, Wu T, Zhang G, Liu S. Highly selective fluorescence sensing of mercury ions over a broad concentration range based on mixed polymeric micelles. *Macromolecules* 2012;45:3939–47.
- [148] Hu J, Dai L, Liu S. Analyte-reactive amphiphilic thermoresponsive diblock copolymer micelles-based multifunctional ratiometric fluorescent chemosensors. *Macromolecules* 2011;44:4699–710.
- [149] Pu KY, Li K, Liu B. A molecular brush approach to enhance quantum yield and suppress nonspecific interactions of conjugated polyelectrolyte for targeted far-red/near-infrared fluorescence cell imaging. *Adv Funct Mater* 2010;20:2770–7.
- [150] Lu H, Su F, Mei Q, Tian Y, Tian W, Johnson RH, Meldrum DR. Using fluorine-containing amphiphilic random copolymers to manipulate the quantum yields of aggregation-induced emission fluorophores in aqueous solutions and the use of these polymers for fluorescent bioimaging. *J Mater Chem* 2012;22:9890–900.
- [151] Lim CK, Kim S, Kwon IC, Ahn CH, Park SY. Dye-condensed biopolymeric hybrids: chromophoric aggregation and self-assembly toward fluorescent bionanoparticles for near infrared bioimaging. *Chem Mater* 2009;21:5819–25.
- [152] Chen JI, Wu WC. Fluorescent polymeric micelles with aggregation-induced emission properties for monitoring the encapsulation of doxorubicin. *Macromol Biosci* 2013;13:623–32.
- [153] Feng X, Tang Y, Duan X, Liu L, Wang S. Lipid-modified conjugated polymer nanoparticles for cell imaging and transfection. *J Mater Chem* 2010;20:1312–6.
- [154] Quan CY, Chen JX, Wang HY, Li C, Chang C, Zhang XZ, Zhuo RX. Core-shell nanosized assemblies mediated by the  $\alpha$ - $\beta$  cyclodextrin dimer with a tumor-triggered targeting property. *ACS Nano* 2010;4:4211–9.
- [155] Petkau K, Kaeser A, Fischer IN, Brunsved L, Schenning AP. Pre-and postfunctionalized self-assembled  $\pi$ -conjugated fluorescent organic nanoparticles for dual targeting. *J Am Chem Soc* 2011;133:17063–71.
- [156] Wang X, Tian X, Zhang Q, Sun P, Wu J, Zhou H, Jin B, Yang J, Zhang S, Wang C. Assembly, two-photon absorption, and bioimaging of living cells of a cuprous cluster. *Chem Mater* 2012;24:954–61.
- [157] Yan Z, Guang SY, Xu HY, Su XY, Ji XL, Liu XY. Supramolecular self-assembly structures and properties of zwitterionic squaraine molecules. *RSC Adv* 2013;3:8021–7.
- [158] Kaiser TE, Wang H, Stepanenko V, Würthner F. Supramolecular construction of fluorescent J-aggregates based on hydrogen-bonded perylene dyes. *Angew Chem Int Ed* 2007;46:5541–4.

- [159] Wang X, Kim YG, Drew C, Ku BC, Kumar J, Samuelson LA. Electrostatic assembly of conjugated polymer thin layers on electrospun nanofibrous membranes for biosensors. *Nano Lett* 2004;4:331–4.
- [160] Li M, Li GL, Zhang Z, Li J, Neoh KG, Kang ET. Self-assembly of pH-responsive and fluorescent comb-like amphiphilic copolymers in aqueous media. *Polymer* 2010;51:3377–86.
- [161] He F, Gädt T, Manners I, Winnik MA. Fluorescent “barcode” multi-block co-micelles via the living self-assembly of di-and triblock copolymers with a crystalline core-forming metalloblock. *J Am Chem Soc* 2011;133:9095–103.
- [162] Tyrrell ZL, Shen Y, Radosz M. Fabrication of micellar nanoparticles for drug delivery through the self-assembly of block copolymers. *Prog Polym Sci* 2010;35:1128–43.
- [163] Chang S, Chiu S, Hsu C, Chang Y, Liu Y. White-light fluorescent nanoparticles from self-assembly of rhodamine B-anchored amphiphilic poly(poly(ethylene glycol) methacrylate)-b-poly(glycidyl methacrylate) block copolymer. *Polymer* 2012;53: 4399–406.
- [164] Zhang B, Wang D, Li M, Li Y, Chen X. Synthesis of star-comb-shaped polymer with porphyrin-core and its self-assembly behavior study. *J Appl Polym Sci* 2012;126:2067–76.
- [165] Cheng F, Bonder EM, Doshi A, Jäkle F. Organoborlon star polymers via arm-first RAFT polymerization: synthesis, luminescent behavior, and aqueous self-assembly. *Polym Chem* 2012;3:596–600.
- [166] Olivier JH, Widmaier J, Ziessl R. Near-infrared fluorescent nanoparticles formed by self-assembly of lipidic (BODIPY) dyes. *Chem Eur J* 2011;17:11709–14.
- [167] Gassensmith JJ, Barr L, Baumes JM, Paek A, Nguyen A, Smith BD. Synthesis and photophysical investigation of squaraine rotaxanes by “clicked capping”. *Org Lett* 2008;10:3343–6.
- [168] Gassensmith JJ, Arunkumar E, Barr L, Baumes JM, DiVittorio KM, Johnson JR, Noll BC, Smith BD. Self-assembly of fluorescent inclusion complexes in competitive media including the interior of living cells. *J Am Chem Soc* 2007;129:15054–9.
- [169] Xu Z, Liao Q, Wu Y, Ren W, Li W, Liu L, Wang S, Gu Z, Zhang H, Fu H. Water-miscible organic J-aggregate nanoparticles as efficient two-photon fluorescent nanoprobe for bioimaging. *J Mater Chem* 2012;22:17737–43.
- [170] Mayer A, Neuenhofer S. Luminescent labels-more than just an alternative to radioisotopes? *Angew Chem Int Ed* 1994;33: 1044–72.
- [171] Luo J, Xie Z, Lam JWY, Cheng L, Chen H, Qiu C, Kwok HS, Zhan X, Liu Y, Zhu D, Tang B. Aggregation-induced emission of 1-methyl-1,2,3,4,5-pentaphenylsilole. *Chem Commun* 2001:1740–1.
- [172] Wang M, Zhang G, Zhang D, Zhu D, Tang B. Fluorescent bio/chemosensors based on silole and tetraphenylethene luminogens with aggregation-induced emission feature. *J Mater Chem* 2010;20:1858–67.
- [173] Hong Y, Lam JW, Tang B. Aggregation-induced emission: phenomenon, mechanism and applications. *Chem Commun* 2009;4332–53.
- [174] Ding D, Li K, Liu B, Tang BZ. Bioprobe based on AIE fluorogens. *Acc Chem Res* 2013, <http://dx.doi.org/10.1021/ar3003464>.
- [175] Chen J, Peng H, Law CC, Dong Y, Lam JW, Williams ID, Tang B. Hyperbranched poly(phenylenesilole)s: synthesis, thermal stability, electronic conjugation, optical power limiting, and cooling-enhanced light emission. *Macromolecules* 2003;36:4319–27.
- [176] Chan PY, Haeussler M, Tang B, Dong Y, Sin KK, Mak WC, Trau D, Seydack M, Renneberg R. Silole nanocrystals as novel biolabels. *J Immunol Methods* 2004;295:111–8.
- [177] Hatano K, Aizawa H, Yokota H, Yamada A, Esumi Y, Koshino H, Koyama T, Matsuoka K, Terunuma D. Highly luminescent glycocluster: silole-core carbosilane dendrimer having peripheral globotriaose. *Tetrahedron Lett* 2007;48:4365–8.
- [178] Yu Y, Feng C, Hong Y, Liu J, Chen S, Ng KM, Luo KQ, Tang B. Cytophilic fluorescent bioprobes for long-term cell tracking. *Adv Mater* 2011;23:3298–302.
- [179] Yu Y, Hong Y, Feng C, Liu J, Lam JWY, Faisal M, Ng KM, Luo KQ, Tang B. Synthesis of an AIE-active fluorogen and its application in cell imaging. *Sci Chin Ser B* 2009;52:15–9.
- [180] Sun F, Zhang G, Zhang D, Xue L, Jiang H. Aqueous fluorescence turn-on sensor for  $Zn^{2+}$  with a tetraphenylethylene compound. *Org Lett* 2011;13:6378–81.
- [181] Hu R, Ye R, Lam JW, Li M, Leung CW, Tang B. Conjugated polyelectrolytes with aggregation-enhanced emission characteristics: synthesis and their biological applications. *Chem Asian J* 2013;8:2436–45.
- [182] Hong Y, Chen S, Leung CWT, Lam JWY, Tang B. Water-soluble tetraphenylethene derivatives as fluorescent “light-up” probes for nucleic acid detection and their applications in cell imaging. *Chem Asian J* 2013;8:1806–12.
- [183] Zhao E, Hong Y, Chen S, Leung CW, Chan CY, Kwok RT, Lam JW, Tang B. Highly fluorescent and photostable probe for long-term bacterial viability assay based on aggregation-induced emission. *Adv Health-care Mater* 2013, <http://dx.doi.org/10.1002/adhm.201200475>.
- [184] Wang Z, Chen S, Lam JW, Qin W, Kwok RT, Xie N, Hu Q, Tang B. Long-term fluorescent cellular tracing by the aggregates of AIE bioconjugates. *J Am Chem Soc* 2013;135:8238–45.
- [185] Qin W, Ding D, Liu J, Yuan W, Hu Y, Liu B, Tang B. Biocompatible nanoparticles with aggregation-induced emission characteristics as far-red/near-infrared fluorescent bioprobes for *in vitro* and *in vivo* imaging applications. *Adv Funct Mater* 2012;22:771–9.
- [186] Wu W, Chen C, Tian Y, Jang SH, Hong Y, Liu Y, Hu R, Tang B, Lee Y, Chen CT. Enhancement of aggregation-induced emission in dye-encapsulating polymeric micelles for bioimaging. *Adv Funct Mater* 2010;20:1413–23.
- [187] He J, Xu B, Chen F, Xia H, Li K, Ye L, Tian W. Aggregation-induced emission in the crystals of 9,10-distyrylanthracene derivatives: the essential role of restricted intramolecular torsion. *J Phys Chem C* 2009;113:9892–9.
- [188] Wang Z, Ma K, Xu B, Li X, Tian W. A highly sensitive “turn-on” fluorescent probe for bovine serum albumin protein detection and quantification based on AIE-active distyrylanthracene derivative. *Sci China Chem* 2013;56:1234–8.
- [189] Lee YD, Lim CK, Singh A, Koh J, Kim J, Kwon IC, Kim S. Dye/peroxalate aggregated nanoparticles with enhanced and tunable chemiluminescence for biomedical imaging of hydrogen peroxide. *ACS Nano* 2012;6:6759–66.
- [190] He F, Xu H, Yang B, Duan Y, Tian L, Huang K, Ma Y, Liu S, Feng S, Shen J. Oligomeric phenylenevinylene with cross dipole arrangement and amorphous morphology: enhanced solid-state luminescence efficiency and electroluminescence performance. *Adv Mater* 2005;17:2710–4.
- [191] An BK, Kwon SK, Jung SD, Park SY. Enhanced emission and its switching in fluorescent organic nanoparticles. *J Am Chem Soc* 2002;124:14410–5.
- [192] Resch Genger U, Grabolle M, Cavaliere Jaricot S, Nitschke R, Nann T. Quantum dots versus organic dyes as fluorescent labels. *Nat Methods* 2008;5:763–75.
- [193] Li JJ, Zhu JJ. Quantum dot for fluorescent biosensing and bioimaging applications. *Analyst* 2013;138:2506–15.
- [194] Hutter E, Maysinger D. Gold nanoparticles and quantum dots for bioimaging. *Microsc Res Tech* 2011;74:592–604.
- [195] Wang Y, Hu R, Lin G, Roy I, Yong KT. Functionalized quantum dots for biosensing and bioimaging and concerns on toxicity. *ACS Appl Mater Interfaces* 2013;5:2786–99.
- [196] Martinez Maestro L, Jacinto C, Rocha U, Carmen Iglesias-de la Cruz M, Sanz-Rodríguez F, Juarranz A, García Solé J, Jaqué D. Optimum quantum dot size for highly efficient fluorescence bioimaging. *J Appl Phys* 2012;111:023513–23516.
- [197] Zrazhevskiy P, Gao X. Multifunctional quantum dots for personalized medicine. *Nano Today* 2009;4:414–28.
- [198] Arya H, Kaul Z, Wadhwa R, Taira K, Hirano T, Kaul SC. Quantum dots in bioimaging: revolution by the small. *Biochem Biophys Res Commun* 2005;329:1173–7.
- [199] Maestro L, Ramírez Hernández J, Bogdan N, Capobianco J, Vetrone F, Solé JG, Jaqué D. Deep tissue bioimaging using two-photon excited CdTe fluorescent quantum dots working within the biological window. *Nanoscale* 2012;4:298–302.
- [200] Wei G, Yan M, Ma L, Zhang H. The synthesis of highly water-dispersible and targeted CdS quantum dots and it is used for bioimaging by confocal microscopy. *Spectrochim Acta A* 2012;85:288–92.
- [201] Yong KT, Law WC, Hu R, Ye L, Liu L, Swihart MT, Prasad PN. Nanotoxicity assessment of quantum dots: from cellular to primate studies. *Chem Soc Rev* 2013;42:1236–50.
- [202] Deng D, Cao J, Qu L, Achilefu S, Gu Y. Highly luminescent water-soluble quaternary Zn–Ag–In–S quantum dots for tumor cell-targeted imaging. *Phys Chem Chem Phys* 2013;15: 5078–83.
- [203] Peng ZA, Peng X. Formation of high-quality CdTe, CdSe, and CdS nanocrystals using CdO as precursor. *J Am Chem Soc* 2001;123:183–4.
- [204] Deng D, Chen Y, Cao J, Tian J, Qian Z, Achilefu S, Gu Y. High-quality CuInS<sub>2</sub>/ZnS quantum dots for *in vitro* and *in vivo* bioimaging. *Chem Mater* 2012;24:3029–37.
- [205] Ye L, Yong KT, Liu L, Roy I, Hu R, Zhu J, Cai H, Law WC, Liu J, Wang K. A pilot study in non-human primates shows no adverse

- response to intravenous injection of quantum dots. *Nat Nanotechnol* 2012;7:453–8.
- [206] Oh JK. Surface modification of colloidal CdX-based quantum dots for biomedical applications. *J Mater Chem* 2010;20:8433–45.
- [207] Wang J, Lu Y, Peng F, Zhong Y, Zhou Y, Jiang X, Su Y, He Y. Photostable water-dispersible NIR-emitting CdTe/CdS/ZnS core–shell–shell quantum dots for high-resolution tumor targeting. *Biomaterials* 2013;34:9509–18.
- [208] Xu B, Cai B, Liu M, Fan H. Ultraviolet radiation synthesis of water dispersed CdTe/CdS/ZnS core–shell–shell quantum dots with high fluorescence strength and biocompatibility. *Nanotechnology* 2013;24, 205601/1–12.
- [209] Feugang JM, Youngblood RC, Greene JM, Fahad AS, Monroe WA, Willard ST, Ryan PL. Application of quantum dot nanoparticles for potential non-invasive bioimaging of mammalian spermatozoa. *J Nanobiotechnol* 2012;10:45–52.
- [210] Wang Q, Xu Y, Zhao X, Chang Y, Liu Y, Jiang L, Sharma J, Seo DK, Yan H. A facile one-step *in situ* functionalization of quantum dots with preserved photoluminescence for bioconjugation. *J Am Chem Soc* 2007;129:6380–1.
- [211] Liu W, Choi HS, Zimmer JP, Tanaka E, Frangioni JV, Bawendi M. Compact cysteine-coated CdSe (ZnCdS) quantum dots for *in vivo* applications. *J Am Chem Soc* 2007;129:14530–1.
- [212] Chan WC, Nie S. Quantum dot bioconjugates for ultrasensitive non-isotopic detection. *Science* 1998;281:2016–8.
- [213] Dubertret B, Skourides P, Norris DJ, Noireaux V, Brivanlou AH, Libchaber A. *In vivo* imaging of quantum dots encapsulated in phospholipid micelles. *Science* 2002;298:1759–62.
- [214] Gao X, Cui Y, Levenson RM, Chung LW, Nie S. *In vivo* cancer targeting and imaging with semiconductor quantum dots. *Nat Biotechnol* 2004;22:969–76.
- [215] Jan'czewski D, Tomczak N, Han MY, Vancso GJ. Stimulus responsive PNIPAM/QD hybrid microspheres by copolymerization with surface engineered QDs. *Macromolecules* 2009;42:1801–4.
- [216] Yang B, Li Y, Sun X, Meng X, Chen P, Liu N. A pH-responsive drug release system based on doxorubicin conjugated amphiphilic polymer coated quantum dots for tumor cell targeting and tracking. *J Chem Technol Biotechnol* 2013, <http://dx.doi.org/10.1002/jctb.4081>.
- [217] Yezhelyev MV, Qi L, O'Regan RM, Nie S, Gao X. Proton-sponge coated quantum dots for siRNA delivery and intracellular imaging. *J Am Chem Soc* 2008;130:9006–12.
- [218] Zhu Y, Li Z, Chen M, Cooper HM, Lu GQ, Xu ZP. Synthesis of robust sandwich-like SiO<sub>2</sub>@CdTe@SiO<sub>2</sub> fluorescent nanoparticles for cellular imaging. *Chem Mater* 2012;24:421–3.
- [219] Selvan S, Patra PK, Ang CY, Ying JV. Synthesis of silica-coated semiconductor and magnetic quantum dots and their use in the imaging of live cells. *Angew Chem* 2007;119:2500–4.
- [220] Malvindi MA, Brunetti V, Vecchio G, Galeone A, Cingolani R, Pompa PP. SiO<sub>2</sub> nanoparticles biocompatibility and their potential for gene delivery and silencing. *Nanoscale* 2012;4:486–95.
- [221] Bardi G, Malvindi MA, Gherardini L, Costa M, Pompa PP, Cingolani R, Pizzorusso T. The biocompatibility of amino functionalized CdSe/ZnS quantum-dot-doped SiO<sub>2</sub> nanoparticles with primary neural cells and their gene carrying performance. *Biomaterials* 2010;31:6555–66.
- [222] English DS, Pell LE, Yu Z, Barbara PF, Korgel BA. Size tunable visible luminescence from individual organic monolayer stabilized silicon nanocrystal quantum dots. *Nano Lett* 2002;2:681–5.
- [223] Rogozhina E, Belomoin G, Smith A, Abu Hassan L, Barry N, Akcakir O, Braun P, Nayfeh M. Si–N linkage in ultrabright, ultrasmall Si nanoparticles. *Appl Phys Lett* 2001;78:3711–3.
- [224] Anderson I, Shirliff R, Macauley C, Smith D, Lee B, Agarwal S, Stradins P, Collins R. Silanization of low-temperature-plasma synthesized silicon quantum dots for production of a tunable, stable, colloidal solution. *J Phys Chem C* 2012;116:3979–87.
- [225] Warner JH, Hoshino A, Yamamoto K, Tilley R. Water-soluble photoluminescent silicon quantum dots. *Angew Chem Int Ed* 2005;44:4550–4.
- [226] Rosso-Vasic M, Spruijt E, van Lagen B, De Cola L, Zuilhof H. Alkyl-functionalized oxide-free silicon nanoparticles: synthesis and optical properties. *Small* 2008;4:1835–41.
- [227] Zou J, Baldwin RK, Pettigrew KA, Kauzlarich SM. Solution synthesis of ultrastable luminescent siloxane-coated silicon nanoparticles. *Nano Lett* 2004;4:1181–6.
- [228] Liu J, Erogogbofo F, Yong KT, Ye L, Liu J, Hu R, Chen H, Hu Y, Yang Y, Yang J. Assessing clinical prospects of silicon quantum dots: studies in mice and monkeys. *ACS Nano* 2013;7:7303–10.
- [229] Romero JJ, Llansola-Portolés MJ, Dell'Arciprete ML, Rodríguez HB, Moore AL, Gonzalez MC. Photoluminescent 1–2 nm size silicon nanoparticles: a surface-dependent system. *Chem Mater* 2013;25:3488–98.
- [230] Rosso-Vasic M, Spruijt E, Popović Z, Overgaag K, van Lagen B, Grandidier B, Vanmaekelbergh D, Domínguez-Gutiérrez D, De Cola L, Zuilhof H. Amine-terminated silicon nanoparticles: synthesis, optical properties and their use in bioimaging. *J Mater Chem* 2009;19:5926–33.
- [231] Zhong Y, Peng F, Bao F, Wang S, Ji X, Yang L, Su Y, Lee ST, He Y. Large-scale aqueous synthesis of fluorescent and biocompatible silicon nanoparticles and their use as highly photostable biological probes. *J Am Chem Soc* 2013;135:8350–6.
- [232] Chinnathambi S, Chen S, Ganeshan S, Hanagata N. Silicon quantum dots for biological applications. *Adv Healthcare Mater* 2013, <http://dx.doi.org/10.1002/adhm.201300157>.
- [233] Park JH, Gu L, von Maltzahn G, Ruoslahti E, Bhatia SN, Sailor MJ. Biodegradable luminescent porous silicon nanoparticles for *in vivo* applications. *Nat Mater* 2009;8:331–6.
- [234] Zheng J, Nicovich PR, Dickson RM. Highly fluorescent noble metal quantum dots. *Annu Rev Phys Chem* 2007;58:409–31.
- [235] Xu H, Suslick KS. Water-soluble fluorescent silver nanoclusters. *Adv Mater* 2010;22:1078–82.
- [236] Díez I, Ras RHA. Fluorescent silver nanoclusters. *Nanoscale* 2011;3:1963–70.
- [237] Bruchez M, Moronne M, Gin P, Weiss S, Alivisatos AP. Semiconductor nanocrystals as fluorescent biological labels. *Science* 1998;281:2013–6.
- [238] Shang L, Dong S, Nienhaus GU. Ultra-small fluorescent metal nanoclusters: synthesis and biological applications. *Nano Today* 2011;6:401–18.
- [239] Lin CAJ, Lee CH, Hsieh JT, Wang HH, Li JK, Shen JL, Chan WH, Yeh HI, Chang WH. Review: synthesis of fluorescent metallic nanoclusters toward biomedical application: recent progress and present challenges. *J Med Biol Eng* 2009;29:276–83.
- [240] Jiang Y, Horimoto NN, Imura K, Okamoto H, Matsui K, Shigemoto R. Bioimaging with two-photon-induced luminescence from triangular nanoplates and nanoparticle aggregates of gold. *Adv Mater* 2009;21:2309–13.
- [241] Eustis S, El-Sayed MA. Why gold nanoparticles are more precious than pretty gold: noble metal surface plasmon resonance and its enhancement of the radiative and nonradiative properties of nanocrystals of different shapes. *Chem Soc Rev* 2006;35:209–17.
- [242] Xie J, Zheng Y, Ying JV. Protein-directed synthesis of highly fluorescent gold nanoclusters. *J Am Chem Soc* 2009;131:888–9.
- [243] Sperling RA, Gil PR, Zhang F, Zanella M, Parak WJ. Biological applications of gold nanoparticles. *Chem Soc Rev* 2008;37:1896–908.
- [244] Choi S, Dickson RM, Yu J. Developing luminescent silver nanodots for biological applications. *Chem Soc Rev* 2012;41:1867–91.
- [245] Giljohann DA, Seferos DS, Prigodich AE, Patel PC, Mirkin CA. Gene regulation with polyvalent siRNA-nanoparticle conjugates. *J Am Chem Soc* 2009;131:2072–3.
- [246] Lin CAJ, Yang TY, Lee CH, Huang SH, Sperling RA, Zanella M, Li JK, Shen JL, Wang HH, Yeh HI. Synthesis, characterization, and bioconjugation of fluorescent gold nanoclusters toward biological labeling applications. *ACS Nano* 2009;3:395–401.
- [247] Huang S, Pfeiffer C, Hollmann J, Friede S, Chen JJC, Beyer A, Haas B, Volz K, Heimbrot W, Montenegro Martos JM. Synthesis and characterization of colloidal fluorescent silver nanoclusters. *Langmuir* 2012;28:8915–9.
- [248] Elbakry A, Zaky A, Liebl R, Rachel R, Goepferich A, Breunig M. Layer-by-layer assembled gold nanoparticles for siRNA delivery. *Nano Lett* 2009;9:2059–64.
- [249] Lee JS, Green JJ, Love KT, Sunshine J, Langer R, Anderson DG. Gold, poly(β-amino ester) nanoparticles for small interfering RNA delivery. *Nano Lett* 2009;9:2402–6.
- [250] Hong R, Han G, Fernández JM, Kim BJ, Forbes NS, Rotello VM. Glutathione-mediated delivery and release using monolayer protected nanoparticle carriers. *J Am Chem Soc* 2006;128:1078–9.
- [251] Ai J, Guo W, Li B, Li T, Li D, Wang E. DNA G-quadruplex-templated formation of the fluorescent silver nanocluster and its application to bioimaging. *Talanta* 2012;88:450–5.
- [252] Shang L, Azadfar N, Stockmar F, Send W, Trouillet V, Bruns M, Gerthsen D, Nienhaus GU. One-pot synthesis of near-infrared fluorescent gold clusters for cellular fluorescence lifetime imaging. *Small* 2011;7:2614–20.
- [253] Wang HH, Lin CAJ, Lee CH, Lin YC, Tseng YM, Hsieh CL, Chen CH, Tsai CH, Hsieh CT, Shen JL. Fluorescent gold nanoclusters as a

- biocompatible marker for in vitro and in vivo tracking of endothelial cells. *ACS Nano* 2011;5:4337–44.
- [254] Rastogi SK, Denn BD, Branen AL. Synthesis of highly fluorescent and thio-linkers stabilize gold quantum dots and nano clusters in DMF for bio-labeling. *J Nanopart Res* 2012;14:1–12.
- [255] Shang L, Dörlisch RM, Brandholt S, Schneider R, Trouillet V, Bruns M, Gerthsen D, Nienhaus GU. Facile preparation of water-soluble fluorescent gold nanoclusters for cellular imaging applications. *Nanoscale* 2011;3:2009–14.
- [256] Liu CL, Wu HT, Hsiao YH, Lai CW, Shih CW, Peng YK, Tang KC, Chang HW, Chien YC, Hsiao JK. Insulin-directed synthesis of fluorescent gold nanoclusters: preservation of insulin bioactivity and versatility in cell imaging. *Angew Chem Int Ed* 2011;50:7056–60.
- [257] Le Guével X, Spies C, Daum N, Jung G, Schneider M. Highly fluorescent silver nanoclusters stabilized by glutathione: a promising fluorescent label for bioimaging. *Nano Res* 2012;5:379–87.
- [258] Qian J, Jiang L, Cai F, Wang D, He S. Fluorescence-surface enhanced Raman scattering co-functionalized gold nanorods as near-infrared probes for purely optical in vivo imaging. *Biomaterials* 2011;32:1601–10.
- [259] Yi DK, Sun IC, Ryu JH, Koo H, Park CW, Youn IC, Choi K, Kwon IC, Kim K, Ahn CH. Matrix metalloproteinase sensitive gold nanorod for simultaneous bioimaging and photothermal therapy of cancer. *Bioconjugate Chem* 2010;21:2173–7.
- [260] Shahjamali MM, Bosman M, Cao S, Huang X, Saadat S, Martinsson E, Aili D, Tay YY, Liedberg B, Loo SCJ. Gold coating of silver nanoprism. *Adv Funct Mater* 2012;22:849–54.
- [261] Bao C, Beziere N, del Pino P, Pelaz B, Estrada G, Tian F, Ntziachristos V, de la Fuente JM, Cui D. Gold nanoprisms as optoacoustic signal nanoamplifiers for in vivo bioimaging of gastrointestinal cancers. *Small* 2013;9:68–74.
- [262] Wang Y, Liu Y, Luehmann H, Xia X, Wan D, Cutler C, Xia Y. Radioluminescent gold nanocages with controlled radioactivity for real-time in vivo imaging. *Nano Lett* 2013;13:581–5.
- [263] Xia Y, Li W, Cobley CM, Chen J, Xia X, Zhang Q, Yang M, Cho EC, Brown PK. Gold nanocages: from synthesis to theranostic applications. *Acc Chem Res* 2011;44:914–24.
- [264] Liang J, Li K, Gurzadyan GG, Lu X, Liu B. Silver nanocube-enhanced far-red/near-infrared fluorescence of conjugated polyelectrolyte for cellular imaging. *Langmuir* 2012;28:11302–9.
- [265] Liu X, Liang S, Nan F, Yang Z, Yu X, Zhou L, Hao Z, Wang Q. Solution-dispersible Au nanocube dimers with greatly enhanced two-photon luminescence and SERS. *Nanoscale* 2013;5: 5368–74.
- [266] Chen J, Yang M, Zhang Q, Cho EC, Cobley CM, Kim C, Glaus C, Wang LV, Welch MJ, Xia Y. Gold nanocages: a novel class of multifunctional nanomaterials for theranostic applications. *Adv Funct Mater* 2010;20:3684–94.
- [267] Khlebtsov N, Dykman L. Biodistribution and toxicity of engineered gold nanoparticles: a review of in vitro and in vivo studies. *Chem Soc Rev* 2011;40:1647–71.
- [268] Haase M, Schäfer H. Upconverting nanoparticles. *Angew Chem Int Ed* 2011;50:5808–29.
- [269] Wang F, Liu X. Recent advances in the chemistry of lanthanide-doped upconversion nanocrystals. *Chem Soc Rev* 2009;38:976–89.
- [270] Wang F, Han Y, Lim CS, Lu Y, Wang J, Xu J, Chen H, Zhang C, Hong M, Liu X. Simultaneous phase and size control of upconversion nanocrystals through lanthanide doping. *Nature* 2010;463:1061–5.
- [271] Zhang F, Che R, Li X, Yao C, Yang J, Shen D, Hu P, Li W, Zhao D. Direct imaging the upconversion nanocrystal core/shell structure at the subnanometer level: shell thickness dependence in upconverting optical properties. *Nano Lett* 2012;12:2852–8.
- [272] Cheng L, Wang C, Liu Z. Upconversion nanoparticles and their composite nanostructures for biomedical imaging and cancer therapy. *Nanoscale* 2013;5:23–7.
- [273] Auzel F. Upconversion and anti-Stokes processes with f and d ions in solids. *Chem Rev* 2004;104:139–74.
- [274] Wang G, Peng Q, Li Y. Lanthanide-doped nanocrystals: synthesis, optical-magnetic properties, and applications. *Acc Chem Res* 2011;44:322–32.
- [275] Zhou J, Liu Z, Li F. Upconversion nanophosphors for small-animal imaging. *Chem Soc Rev* 2011;41:1323–49.
- [276] Hilderbrand SA, Shao F, Salthouse C, Mahmood U, Weissleder R. Upconverting luminescent nanomaterials: application to in vivo bioimaging. *Chem Commun* 2009;4188–90.
- [277] Yin W, Zhao L, Zhou L, Gu Z, Liu X, Tian G, Jin S, Yan L, Ren W, Xing G. Enhanced red emission from  $\text{GdF}_3:\text{Yb}^{3+}, \text{Er}^{3+}$  upconversion nanocrystals by  $\text{Li}^+$  doping and their application for bioimaging. *Chem Eur J* 2012;18:9239–45.
- [278] Yang D, Kang X, Ma P, Dai Y, Hou Z, Cheng Z, Li C, Lin J. Hollow structured upconversion luminescent  $\text{NaYF}_4:\text{Yb}^{3+}, \text{Er}^{3+}$  nanospheres for cell imaging and targeted anti-cancer drug delivery. *Biomaterials* 2013;34:1601–12.
- [279] Yang Y, Sun Y, Cao T, Peng J, Liu Y, Wu Y, Feng W, Zhang Y, Li F. Hydrothermal synthesis of  $\text{NaLuF}_4:\text{Sm}, \text{Yb}, \text{Tm}$  nanoparticles and their application in dual-modality upconversion luminescence and SPECT bioimaging. *Biomaterials* 2012;34:774–83.
- [280] Chen G, Shen J, Ohulchansky TY, Patel NJ, Kutikov A, Li Z, Song J, Pandey RK, Ågren H, Prasad PN.  $(\alpha\text{-NaYbF}_4:\text{Tm}^{3+})/\text{CaF}_2$  core/shell nanoparticles with efficient near-infrared to near-infrared upconversion for high-contrast deep tissue bioimaging. *ACS Nano* 2012;6:8280–7.
- [281] Bogdan N, Rodríguez EM, Sanz-Rodríguez F, Juarranz A, Jaque D, Sole JG, Capobianco J. Bio-functionalization of ligand-free upconverting lanthanide doped nanoparticles for bioimaging and cell targeting. *Nanoscale* 2012;4:3647–50.
- [282] Mader HS, Kele P, Saleh SM, Wolfbeis OS. Upconverting luminescent nanoparticles for use in bioconjugation and bioimaging. *Curr Opin Chem Biol* 2010;14:582–96.
- [283] Nyk M, Kumar R, Ohulchansky TY, Bergey EJ, Prasad PN. High contrast in vitro and in vivo photoluminescence bioimaging using near infrared to near infrared up-conversion in  $\text{Tm}^{3+}$  and  $\text{Yb}^{3+}$  doped fluoride nanophosphors. *Nano Lett* 2008;8:3834–8.
- [284] Liu Q, Sun Y, Yang T, Feng W, Li C, Li F. Sub-10 nm hexagonal lanthanide-doped  $\text{NaLuF}_4$  upconversion nanocrystals for sensitive bioimaging in vivo. *J Am Chem Soc* 2011;133:17122–5.
- [285] Liu Q, Yang T, Feng W, Li F. Blue-emissive upconversion nanoparticles for low-power-excited bioimaging in vivo. *J Am Chem Soc* 2012;134:5390–7.
- [286] Zhang Z, Zhang P, Guo K, Liang G, Chen H, Liu B, Kong J. Facile synthesis of fluorescent  $\text{Au}@\text{SiO}_2$  nanocomposites for application in cellular imaging. *Talanta* 2011;85:2695–9.
- [287] Abdul Jalil R, Zhang Y. Biocompatibility of silica coated  $\text{NaYF}_4$  upconversion fluorescent nanocrystals. *Biomaterials* 2008;29: 4122–8.
- [288] Kang X, Cheng Z, Li C, Yang D, Shang M, Ma Pa, Li G, Liu N, Lin J. Core-shell structured up-conversion luminescent and mesoporous  $\text{NaYF}_4:\text{Yb}^{3+}/\text{Er}^{3+}@n\text{SiO}_2@m\text{SiO}_2$  nanospheres as carriers for drug delivery. *J Phys Chem C* 2011;115:15801–11.
- [289] Cho M, Lim K, Woo K. Facile synthesis and optical properties of colloidal silica microspheres encapsulating a quantum dot layer. *Chem Commun* 2010;46:5584–6.
- [290] Jun BH, Hwang DW, Jung HS, Jang J, Kim H, Kang H, Kang T, Kyeong S, Lee H, Jeong DH. Ultrasensitive, biocompatible, quantum-dot-embedded silica nanoparticles for bioimaging. *Adv Funct Mater* 2012;22:1843–9.
- [291] Liu W, Gretyak AB, Lee J, Wong CR, Park J, Marshall LF, Jiang W, Curtin PN, Ting AY, Nocera DG. Compact biocompatible quantum dots via RAFT-mediated synthesis of imidazole-based random copolymer ligand. *J Am Chem Soc* 2009;132:472–83.
- [292] Zhang P, Liu W.  $\text{ZnO QD}@\text{PMAA-co-PDMAEMA}$  nonviral vector for plasmid DNA delivery and bioimaging. *Biomaterials* 2010;31:3087–94.
- [293] Bencherif SA, Siegwart DJ, Srinivasan A, Horkay F, Hollinger JO, Washburn NR, Matyjaszewski K. Nanostructured hybrid hydrogels prepared by a combination of atom transfer radical polymerization and free radical polymerization. *Biomaterials* 2009;30: 5270–8.
- [294] Lin Y, Zhang L, Yao W, Qian H, Ding D, Wu W, Jiang X. Water-soluble chitosan-quantum dot hybrid nanospheres toward bioimaging and biolabeling. *ACS Appl Mater Interfaces* 2011;3:995–1002.
- [295] Wu W, Shen J, Banerjee P, Zhou S. A multifunctional nanoplatform based on responsive fluorescent plasmonic  $\text{ZnO-Au}@\text{PEG}$  hybrid nanogels. *Adv Funct Mater* 2011;21:2830–9.
- [296] Yong KT, Roy I, Hu R, Ding H, Cai H, Zhu J, Zhang X, Bergey EJ, Prasad PN. Synthesis of ternary  $\text{CuInS}_2/\text{ZnS}$  quantum dot bioconjugates and their applications for targeted cancer bioimaging. *Integr Biol* 2010;2:121–9.
- [297] Fan H, Leve EW, Scullin C, Gabaldon J, Tallant D, Bunge S, Boyle T, Wilson MC, Brinker CJ. Surfactant-assisted synthesis of water-soluble and biocompatible semiconductor quantum dot micelles. *Nano Lett* 2005;5:645–8.
- [298] Hu R, Law WC, Lin G, Ye L, Liu J, Reynolds JL, Yong KT. PEGylated phospholipid micelle-encapsulated near-infrared  $\text{PbS}$  quantum dots for in vitro and in vivo bioimaging. *Theranostics* 2012;2:723–33.
- [299] Kainz QM, Schätz A, Zöpfel A, Stark WJ, Reiser O. Combined covalent and noncovalent functionalization of nanomagnetic carbon

- surfaces with dendrimers and BODIPY fluorescent dye. *Chem Mater* 2011;23:3606–13.
- [300] Jao YC, Chen MK, Lin SY. Enhanced quantum yield of dendrimer-entrapped gold nanodots by a specific ion-pair association and microwave irradiation for bioimaging. *Chem Commun* 2010;46: 2626–8.
- [301] Lesniak W, Bielinska AU, Sun K, Janczak KW, Shi X, Baker JR, Balogh LP. Silver/dendrimer nanocomposites as biomarkers: fabrication, characterization, in vitro toxicity, and intracellular detection. *Nano Lett* 2005;5:2123–30.
- [302] Chen Q, Li K, Wen S, Liu H, Peng C, Cai H, Shen M, Zhang G, Shi X. Targeted CT/MR dual mode imaging of tumors using multifunctional dendrimer-entrapped gold nanoparticles. *Biomaterials* 2013;34:5200–9.
- [303] Alcalá MA, Shade CM, Uh H, Kwan SY, Bischof M, Thompson ZP, Gogick KA, Meier AR, Strein TG, Bartlett DL. Preferential accumulation within tumors and *in vivo* imaging by functionalized luminescent dendrimer lanthanide complexes. *Biomaterials* 2011;32: 9343–52.
- [304] Alcalá MA, Kwan SY, Shade CM, Lang M, Uh H, Wang M, Weber SG, Bartlett DL, Petoud S, Lee YJ. Luminescence targeting and imaging using a nanoscale generation 3 dendrimer in an *in vivo* colorectal metastatic rat model. *Nanomed Nanotechnol Biol Med* 2011;7:249–58.
- [305] Govindaraj A, Hwang T, Yoo H, Kim YS, Lee SJ, Choi SW, Kim JH. Synthesis and characterization of multifunctional  $\text{Fe}_3\text{O}_4/\text{poly}(\text{fluorescein O-methacrylate})$  core/shell nanoparticles. *J Colloid Interface Sci* 2012;379:27–32.
- [306] Ma K, Sai H, Wiesner U. Ultrasmall sub-10 nm near-infrared fluorescent mesoporous silica nanoparticles. *J Am Chem Soc* 2012;134:13180–3.
- [307] Bonacchi S, Genovese D, Juris R, Montalti M, Prodi L, Rampazzo E, Sgarci M, Zaccheroni N. Luminescent chemosensors based on silica nanoparticles. *Top Curr Chem* 2011;300:93–138.
- [308] Kumar R, Roy I, Ohulchanskyy TY, Goswami LN, Bonoju AC, Bergey EJ, Trampusch KM, Maitra A, Prasad PN. Covalently dye-linked, surface-controlled, and bioconjugated organically modified silica nanoparticles as targeted probes for optical imaging. *ACS Nano* 2008;2:449–56.
- [309] Zhu H, Tao J, Wang W, Zhou Y, Li P, Li Z, Yan K, Wu S, Yeung KWK, Xu Z. Magnetic, fluorescent, and thermo-responsive  $\text{Fe}_3\text{O}_4$ /rare earth incorporated poly(St-NIPAM) core-shell colloidal nanoparticles in multimodal optical/magnetic resonance imaging probes. *Biomaterials* 2012;34:2296–306.
- [310] Liu J, He W, Zhang L, Zhang Z, Zhu J, Yuan L, Chen H, Cheng Z, Zhu X. Bifunctional nanoparticles with fluorescence and magnetism via surface-initiated AGET ATRP mediated by an iron catalyst. *Langmuir* 2011;27:12684–92.
- [311] Pfaff A, Schallon A, Ruhland TM, Majewski AP, Schmalz H, Freitag R, Müller AH. Magnetic and fluorescent glycopolymer hybrid nanoparticles for intranuclear optical imaging. *Biomacromolecules* 2011;12:3805–11.
- [312] Lu X, Jiang R, Fan Q, Zhang L, Zhang H, Yang M, Ma Y, Wang L, Huang W. Fluorescent-magnetic poly(poly(ethyleneglycol) monomethacrylate)-grafted  $\text{Fe}_3\text{O}_4$  nanoparticles from post-atom-transfer-radical-polymerization modification: synthesis, characterization, cellular uptake and imaging. *J Mater Chem* 2012;22:6965–73.
- [313] Yuan Q, Lee E, Yeudall WA, Yang H. Dendrimer-triglycine-EGF nanoparticles for tumor imaging and targeted nucleic acid and drug delivery. *Oral Oncol* 2010;46:698–704.
- [314] Wang X, Liu H, Chen D, Meng X, Liu T, Fu C, Hao N, Zhang Y, Wu X, Ren J. Multifunctional  $\text{Fe}_3\text{O}_4@\text{P(St/MAA)}$ @Chitosan@Au core/shell nanoparticles for dual imaging and photothermal therapy. *ACS Appl Mater Interfaces* 2013;5:4966–71.
- [315] Choi JH, Kang SR, Kim H, Um SH, Shin K, Choi JW, Oh BK. Dye-doped silica nanoparticle with HIV-1 TAT peptide for bioimaging. *J Biomed Nanotechnol* 2013;9:291–4.
- [316] Lee CS, Chang HH, Jung J, Lee NA, Song NW, Chung BH. A novel fluorescent nanoparticle composed of fluorene copolymer core and silica shell with enhanced photostability. *Colloids Surf B Biointerfaces* 2012;91:219–25.
- [317] Zhao J, Liu Y, Park HJ, Boggs JM, Basu A. Carbohydrate-coated fluorescent silica nanoparticles as probes for the galactose/β-sulfogalactose carbohydrate-carbohydrate interaction using model systems and cellular binding studies. *Bioconjugate Chem* 2012;23:1166–73.
- [318] Sun HT, Yang J, Fujii M, Sakka Y, Zhu Y, Asahara T, Shirahata N, Li M, Bai Z, Li JG. Highly fluorescent silica-coated bismuth-doped aluminosilicate nanoparticles for near-infrared bioimaging. *Small* 2011;7:199–203.
- [319] Bae SW, Tan W, Hong JI. Fluorescent dye-doped silica nanoparticles: new tools for bioapplications. *Chem Commun* 2012;48: 2270–82.
- [320] Qiu F, Zhu Q, Tong G, Zhu L, Wang D, Yan D, Zhu X. Highly fluorescent core-shell hybrid nanoparticles templated by unimolecular star conjugated polymer for biological tool. *Chem Commun* 2012;48:11954–6.
- [321] Li M, Lam JWY, Faisal M, Chen S, Zhang W, Hong Y, Xiong J, Zheng Q, Tang BZ. Biotin-decorated fluorescent silica nanoparticles with aggregation-induced emission characteristics: fabrication, cytotoxicity and biological applications. *J Mater Chem B* 2013;1:676–84.
- [322] Zhao Q, Li F, Huang C. Phosphorescent chemosensors based on heavy-metal complexes. *Chem Soc Rev* 2010;39:3007–30.
- [323] Yang Y, Zhao Q, Feng W, Li F. Luminescent chemodosimeters for bioimaging. *Chem Rev* 2012;113:192–270.
- [324] Zhao Q, Huang C, Li F. Phosphorescent heavy-metal complexes for bioimaging. *Chem Soc Rev* 2011;40:2508–24.
- [325] Li C, Liu Y, Wu Y, Sun Y, Li F. The cellular uptake and localization of non-emissive iridium (III) complexes as cellular reaction-based luminescence probes. *Biomaterials* 2012;34:1223–34.
- [326] Tan W, Zhou J, Li F, Yi T, Tian H. Visible light-triggered photoswitchable diarylethene-based iridium(III) complexes for imaging living cells. *Chem Asian J* 2011;6:1263–8.
- [327] Shi H, Sun H, Yang H, Liu S, Jenkins G, Feng W, Li F, Zhao Q, Liu B, Huang W. Cationic polyfluoranes with phosphorescent Iridium(III) complexes for time-resolved luminescent biosensing and fluorescence lifetime imaging. *Adv Funct Mater* 2013;23:3268–76.
- [328] Sharma P, Brown S, Walter G, Santra S, Moudgil B. Nanoparticles for bioimaging. *Adv Colloid Interface Sci* 2006;123:471–85.
- [329] Klostranec JM, Chan WC. Quantum dots in biological and biomedical research: recent progress and present challenges. *Adv Mater* 2006;18:1953–64.
- [330] Chen Z, Chen H, Meng H, Xing G, Gao X, Sun B, Shi X, Yuan H, Zhang C, Liu R. Bio-distribution and metabolic paths of silica coated CdSeS quantum dots. *Toxicol Appl Pharmacol* 2008;230:364–71.
- [331] Tiwari DK, Jin T, Behari J. Bio-distribution toxicity assessment of intravenously injected anti-HER2 antibody conjugated CdSe/ZnS quantum dots in Wistar rats. *Int J Nanomed* 2011;6:463–75.
- [332] Su Y, Peng F, Jiang Z, Zhong Y, Lu Y, Jiang X, Huang Q, Fan C, Lee ST, He Y. In vivo distribution, pharmacokinetics, and toxicity of aqueous synthesized cadmium-containing quantum dots. *Biomaterials* 2011;32:5855–62.
- [333] Kim KS, Hur W, Park SJ, Hong SW, Choi JE, Goh EJ, Yoon SK, Hahn SK. Bioimaging for targeted delivery of hyaluronic acid derivatives to the livers in cirrhotic mice using quantum dots. *ACS Nano* 2010;4:3005–14.
- [334] Liu Y, Chen M, Cao T, Sun Y, Li C, Liu Q, Yang T, Yao L, Feng W, Li F. A cyanine-modified nanosystem for in vivo upconversion luminescence bioimaging of methylmercury. *J Am Chem Soc* 2013;135:9869–76.
- [335] Kim S, Lim YT, Soltesz EG, De Grand AM, Lee J, Nakayama A, Parker JA, Mihaljevic T, Laurence RG, Dor DM. Near-infrared fluorescent type II quantum dots for sentinel lymph node mapping. *Nat Biotechnol* 2003;22:93–7.
- [336] Kobayashi H, Hama Y, Koyama Y, Barrett T, Regino CA, Urano Y, Choyke PL. Simultaneous multicolor imaging of five different lymphatic basins using quantum dots. *Nano Lett* 2007;7:1711–6.
- [337] Santra S, Yang H, Dutta D, Stanley JT, Holloway PH, Tan W, Moudgil BM, Mericle RA. TAT conjugated, FITC doped silica nanoparticles for bioimaging applications. *Chem Commun* 2004;2810–1.
- [338] Guo SR, Gong JY, Jiang P, Wu M, Lu Y, Yu SH. Biocompatible, luminescent silver@phenol formaldehyde resin core/shell nanospheres: large-scale synthesis and application for *in vivo* bioimaging. *Adv Funct Mater* 2008;18:872–9.
- [339] Hara M, Murakami T, Kobayashi E. In vivo bioimaging using photogenic rats: fate of injected bone marrow-derived mesenchymal stromal cells. *J Autoimmun* 2008;30:163–71.
- [340] Hu SH, Chen Y, Hung W, Chen IW, Chen S. Quantum-dot-tagged reduced graphene oxide nanocomposites for bright fluorescence bioimaging and photothermal therapy monitored *in situ*. *Adv Mater* 2012;24:1748–54.
- [341] Ahmed E, Morton SW, Hammond PT, Swager TM. Fluorescent multiblock π-conjugated polymer nanoparticles for *in vivo* tumor targeting. *Adv Mater* 2013;34:4786–93.
- [342] Wen CJ, Sung CT, Aljuffali IA, Huang Y, Fang J. Nanocomposite liposomes containing quantum dots and anticancer drugs for bioimaging and therapeutic delivery: a comparison of cationic,

- PEGylated and deformable liposomes. *Nanotechnology* 2013;24:325101/1–13.
- [343] Wu H, Zhang S, Zhang J, Liu G, Shi J, Zhang L, Cui X, Ruan M, He Q, Bu W. A hollow-core, magnetic, and mesoporous double-shell nanostructure: *in situ* decomposition/reduction synthesis, bioimaging, and drug-delivery properties. *Adv Funct Mater* 2011;21:1850–62.
- [344] Wu L, Luderer M, Yang X, Swain C, Zhang H, Nelson K, Stacy AJ, Shen B, Lanza GM, Pan D. Surface passivation of carbon nanoparticles with branched macromolecules influences near infrared bioimaging. *Theranostics* 2013;3:677–86.
- [345] Yang Y, An F, Liu Z, Zhang X, Zhou M, Li W, Hao X, Lee C-S, Zhang X. Ultrabright and ultrastable near-infrared dye nanoparticles for *in vitro* and *in vivo* bioimaging. *Biomaterials* 2012;33:7803–9.
- [346] Cova L, Bigini P, Diana V, Sitia L, Ferrari R, Pesce RM, Khalaf R, Bossolasco P, Ubezio P, Lupi M. Biocompatible fluorescent nanoparticles for *in vivo* stem cell tracking. *Nanotechnology* 2013;24:245603/1–11.
- [347] Kim S, Noh JY, Kim KY, Kim JH, Kang HK, Nam SW, Kim SH, Park S, Kim C, Kim J. Salicylimine-based fluorescent chemosensor for aluminum ions and application to bioimaging. *Inorg Chem* 2012;51:3597–602.
- [348] Wen CJ, Zhang L, Al-Suwayeh SA, Yen TC, Fang JY. Theranostic liposomes loaded with quantum dots and apomorphine for brain targeting and bioimaging. *Int J Nanomed* 2012;7:1599–611.
- [349] Hollis CP, Weiss HL, Leggas M, Evers BM, Gemeinhart RA, Li T. Biodistribution and bioimaging studies of hybrid paclitaxel nanocrystals: lessons learned of the EPR effect and image-guided drug delivery. *J Control Release* 2013;172:12–21.
- [350] Ding D, Liu J, Feng G, Li K, Hu Y, Liu B. Bright far-red/near-infrared conjugated polymer nanoparticles for *in vivo* bioimaging. *Small* 2013;9:3093–102.
- [351] Abdukayum A, Chen J, Zhao Q, Yan X. Functional near infrared-emitting Cr<sup>3+</sup>/Pr<sup>3+</sup> Co-doped zinc gallogermanate persistent luminescent nanoparticles with super-long afterglow for *in vivo* targeted bioimaging. *J Am Chem Soc* 2013;135:14125–33.
- [352] Larson DR, Zipfel WR, Williams RM, Clark SW, Bruchez MP, Wise FW, Webb WW. Water-soluble quantum dots for multiphoton fluorescence imaging *in vivo*. *Science* 2003;300:1434–6.
- [353] Erathodiyl N, Ying JY. Functionalization of inorganic nanoparticles for bioimaging applications. *Acc Chem Res* 2011;44:925–35.
- [354] Wei H, Cheng SX, Zhang XZ, Zhuo RX. Thermo-sensitive polymeric micelles based on poly(N-isopropylacrylamide) as drug carriers. *Prog Polym Sci* 2009;34:893–910.
- [355] Xiao W, Chen WH, Xu XD, Li C, Zhang J, Zhuo RX, Zhang XZ. Design of a cellular-uptake-shielding “plug and play” template for photo controllable drug release. *Adv Mater* 2011;23:3526–30.
- [356] Zhang Y, Yang J. Design strategies for fluorescent biodegradable polymeric biomaterials. *J Mater Chem B* 2013;1:132–48.
- [357] Martinsone Ž, Baķe M. Toxic effects of nanoparticles—differences and similarities with fine particles. *Proc Latvian Acad Sci Sect B* 2010;64:1–9.
- [358] Fischer HC, Chan WC. Nanotoxicity: the growing need for *in vivo* study. *Curr Opin Biotechnol* 2007;18:565–71.
- [359] Winnik FM, Maysinger D. Quantum dot cytotoxicity and ways to reduce it. *Acc Chem Res* 2013;46:672–80.
- [360] Chen N, He Y, Su Y, Li X, Huang Q, Wang H, Zhang X, Tai R, Fan C. The cytotoxicity of cadmium-based quantum dots. *Biomaterials* 2012;33:1238–44.
- [361] Handy R, Shaw B. Toxic effects of nanoparticles and nanomaterials: implications for public health, risk assessment and the public perception of nanotechnology. *Health Risk Soc* 2007;9:125–44.
- [362] Smith AM, Mancini MC, Nie S. Bioimaging: second window for *in vivo* imaging. *Nat Nanotechnol* 2009;4:710–1.